The Report Committee for Sahil Malhotra
Certifies that this is the approved version of the following report:

Proppant Settling in Viscoelastic Surfactant (VES) Fluids

APPROVED BY
SUPERVISING COMMITTEE:

Supervisor: _____
Mukul M. Sharma

_____
Kishore K. Mohanty

Proppant Settling in Viscoelastic Surfactant (VES) Fluids

by

Sahil Malhotra, B.Tech

Report

Presented to the Faculty of the Graduate School of

The University of Texas at Austin

in Partial Fulfillment

of the Requirements

for the Degree of

Master of Science in Engineering

The University of Texas at Austin

December 2010

Acknowledgements

I would like to express my sincere gratitude to Dr. Mukul M. Sharma for his supervision and support throughout the duration of the research project. He has been a great source of inspiration and has helped with all aspects of graduate studies. I would like to thank Dr. Kishore K. Mohanty for reading this report and providing useful suggestions. I would like to appreciate valuable insights by Dr. Satya Gupta of BJ Services.

I would like to thank Glen Baum, Gary Miscoe and Tony Bermudez for helping me with the experimental setup and material procurement. I would also like to thank Roger Terzian for helping with computer installations and software updates. I would like to acknowledge the technical support from the members of the Fracturing and Sand Control Research team: Dr. Kyle Friehauf, Dr. Ajay Suri, Nicolas Roussel, Lionel Ribeiro, Karn Agarwal, Ripudaman Manchanda, Somnath Mondal, Himanshu Yadav and Amos Kim.

My family members and especially my parents have been a great inspiration and I would like to thank them for supporting me. I would also like to thank my friends Abhishek, Abhinav, Divya, Bhargavi, Puja, Purva and Pranav for making the journey enjoyable.

December 2010

Abstract

Proppant Settling in Viscoelastic Surfactant (VES) Fluids

Sahil Malhotra, M. S. E.

The University of Texas at Austin, 2010

Supervisor: Mukul M. Sharma

Polymer-free viscoelastic surfactant-based (VES) fluid systems have been used to eliminate polymer-based damage and to efficiently transport proppants into the fracture. Current models and correlations neglect the important influence of fracture walls and fluid elasticity on proppant settling. This report presents an experimental study that investigates the impact of fluid elasticity and fracture width on proppant settling in VES fluid systems.

Proppant settling experiments are performed in shear-thinning VES fluids. Experimental data is presented to show that fluid elasticity plays an important role in controlling the settling rate of the proppants. It is shown that elastic effects can increase as well as reduce the settling velocities depending upon the rheological properties of the fluid and properties of the proppants. Data is presented to show that the settling velocity

reduces significantly as the proppant size becomes comparable to the fracture width. The reduction in settling velocity due to the presence of the fracture walls depends on the rheological properties of the fluid, ratio of particle diameter to fracture width as well as the diameter of the particle.

Table of Contents

List of Tables

List of Figures

Chapter 1: Introduction

In hydraulic fracturing treatments proppants are placed in the fracture by mixing them with the fracturing fluid. Ideally this fluid is required to have excellent proppant carrying abilities so as to keep the proppants from settling and distribute them uniformly along the length of the fracture. The productivity of fractured wells is determined by two main factors, fracture conductivity and propped fracture length. Both of these factors are very much dependent on effective transport of proppants inside the fracture

A typical hydraulic fracturing treatment proceeds in the following sequence of events: (1) a fluid pad without any proppant, known as the “pad”, is pumped under high pressure to initiate and extend the fracture. (2) The pad is followed by a high-viscosity fluid laden with proppants. The proppants are carried into the fracture due to the high viscosity of this fluid. (3) The third stage or over-flush consists of a fluid without the proppants. The function of the over-flush is to clear the wellbore of any proppant-slurry and displace it into the fracture.

Upon the cessation of pumping the fracture closes on the proppant pack, which provides a highly conducive pathway for the hydrocarbons to flow from the reservoir to the wellbore. For the efficient flow of the hydrocarbons it is required that the proppants are carried far into the fracture, leading to large propped fracture length and these settle uniformly throughout the length of the fracture. The transport of proppants is thus a key issue and it is dependent on many factors including fluid rheology and proppant size, density and concentration as well as fracture width.

In the industry various types of fracturing fluids have been used for hydraulic fracturing operations. These range from conventional fracturing fluids which include water-based and polymer-containing fluids, energized fluids and foams and hydrocarbon-based fluids. Dantas et al. (2005) provides a thorough review of the several types of conventional fracturing fluids and the methodologies applied for their design. The unconventional fracturing fluids include polymer-free fluids, methanol-containing fluids, liquid CO_2 based fluids and liquefied-petroleum based fluids. A review of the unconventional fracturing fluids and their applications can be found in Gupta (2009).

The surfactant based viscoelastic (VES) fluid systems fall under the category of polymer-free fluids and have been widely used for hydraulic fracturing operations (Samuel et al. 1997; Mathis et al. 2002; Leitzell 2007) over the past years. Free of polymers, these fluids leave no residue and facilitate rapid flowback. The operational simplicity of these fluids also provides an advantage over conventional fracturing fluids (Gupta 2009). For VES fluids, elasticity plays an important role in suspending the proppants. It has been pointed out by Asadi et al. (2002) that the zero shear viscosity is an important parameter for evaluating proppant transport in these fluids. However, there is very little data which shows the influence of fluid elasticity on the settling velocity of proppants in VES fluids.

This report provides a review of the past work on proppant settling in viscoelastic fracturing fluids and experimental investigation of proppant settling in VES fluids. Experimental data is presented to show the effect of elasticity on the settling velocities of proppants in these fluids.

Chapter 2: Viscoelastic Behavior of Fluids

2.1 MAXWELL REPRESENTATION

A material which regains its original configuration upon the removal of the stress is a perfectly elastic material. For a perfectly viscous material shear stress is proportional to the shear strain. Viscoelastic fluids exhibit the properties of viscous as well as elastic substances. The most common representation of a viscoelastic fluid as proposed by Maxwell is shown in Figure 2.1.

The figure shows a dashpot which represents the viscous component and a spring which represents the elastic component. The constitutive equation for the Maxwell model is given by:

$$\frac{d\varepsilon}{dt} = \frac{1}{k}\frac{d\tau}{dt} + \frac{\tau}{\eta} \tag{2.1}$$

In this equation τ is the stress in the Maxwell element, ε is the total strain, k is the spring constant of the spring and η is the viscosity of the dashpot. A characteristic relaxation time, T of the Maxwell fluid can be defined as:

$$T = \frac{\eta}{k} \tag{2.2}$$

The relaxation time is the measure of the elasticity of the sample. The higher the relaxation time, the more elastic the behavior of the material. A fluid with a zero relaxation time is a purely viscous (inelastic) fluid.

2.2 RHEOLOGICAL CHARACTERIZATION

The rheological characterization of viscoelastic fluids involves the measurement of the viscosity as well as the elasticity (relaxation time) of the fluid. Different kinds of experimental techniques have been used for the determination of the rheological properties of viscoelastic fluids (Ferry 1970). This section entails the theoretical basis behind the experimental techniques employed in this study.

2.2.1 Steady State Sweep Test for Viscosity Determination

Viscosity can be measured using a conventional rotational viscometer using the double wall Couette geometry. A constant shear strain is applied on the sample by rotating the outer cylinder and the torque on the inner cylinder is measured. The viscosity of the sample can be calculated from the torque generated at steady state. For a non-Newtonian fluid for which viscosity is a function of shear rate, the shear rate on the sample is varied in steps and the viscosity can be calculated at different shear rates. This test is referred to as the Steady State Sweep test. Figure 2.2 shows a schematic of a generalized shear-thinning fluid i.e. the viscosity decreases with increasing shear rates.

2.2.2 Stress Relaxation Test to Measure Relaxation Time

The relaxation time of the fluid can be measured by performing either a Stress Relaxation test or a Dynamic Frequency Sweep test. In a stress relaxation test, a constant strain is instantaneously applied to the sample and the stress generated in the sample is measured as a function of time. For a Maxwell element the stress generated for a constant strain input ε_o can be calculated from the constitutive equation (Equation (2.2)) and is given by:

$$\sigma(t) = 2\varepsilon_0 k\, e^{-\frac{t}{T}} \tag{2.3}$$

The relaxation modulus of the sample can thus be written as

$$E(t) = \frac{\sigma(t)}{\varepsilon_o} = 2k\, e^{-\frac{t}{T}} \tag{2.4}$$

Figure 2.3 shows this stress output for a constant strain input for a viscoelastic material. The relaxation time, T of the sample can thus be calculated by fitting the experimental data for the stress output or the relaxation modulus data to Equation (2.3) or (2.4) respectively.

However, it is important to mention that in fluids the stress decays very rapidly and it can be challenging to measure the stress response accurately in the experiment. In order to avoid this inaccuracy the relaxation time of fluids is generally measured using dynamic tests.

2.2.3 Dynamic Frequency Sweep Test to Measure Relaxation Time

In a dynamic test a sinusoidal shear strain of a particular angular frequency, ω is applied to sample and the stress generated in the sample. For a perfectly elastic material the stress in completely in-phase with the strain and in a perfectly viscous material the stress is completely out-of –phase with the strain. In a viscoelastic material the stress leads the strain by a phase angle, δ (less than 90°). Figure 2.4 shows the stress response for a sinusoidal strain input.

The output stress, σ can be resolved into two components: a component in-phase with the strain, σ' and a component out-of-phase with strain, σ''. Thus, the dynamic modulus, G^* of the sample can be represented as

$$G^* = G' + iG'' \tag{2.5}$$

In this equation $G' = \sigma'/\varepsilon$ is the in-phase component referred to as the elastic modulus or the storage modulus and $G'' = \sigma''/\varepsilon$ is the out-of-phase component referred to as the viscous modulus or the loss modulus.

For a Maxwell model the stress output for a sinusoidal strain input can be calculated by solving the constitutive equation (Equation (2.1)) and using the principle of superposition and linearity to arrive at the following expression for the dynamic modulus:

$$G^*(\omega) = \frac{k\omega^2}{\frac{1}{T^2}+\omega^2} + i\frac{\frac{k\omega}{T}}{\frac{1}{T^2}+\omega^2} \tag{2.6}$$

Using Equations (2.5) and (2.6) we can write:

$$\frac{G''(\omega)}{G'(\omega)} = \frac{1}{\omega T} \tag{2.7}$$

The dynamic test is performed over a range of frequencies, thus referred to as the Dynamic Frequency Sweep Test and the storage and loss moduli are measured as a function of the angular frequency. The Maxwellian relaxation time of the fluid sample can thus be calculated by fitting the experimental moduli, $G'(\omega)$ and $G''(\omega)$ to Equation (2.7).

It is important to note that the above two methods to measure the relaxation time of fluids should be used only if the experimental data fits the Maxwell model. In case the Maxwell model is not fit to represent the experimental data, one relaxation time is not sufficient to quantify the elastic properties of the fluid and a spectrum (multiple) of relaxations times using a Generalized Maxwell model is required (Ferry 1970; Delshad et al. 2008; Kim et al. 2010). The relaxation time which is comparable (in terms of the order of magnitude) to the experimental/process time should then be used for further analysis.

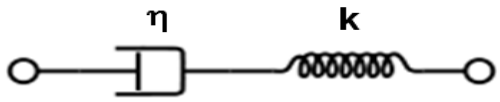

Figure 2.1: Maxwell representation of a viscoelastic fluid

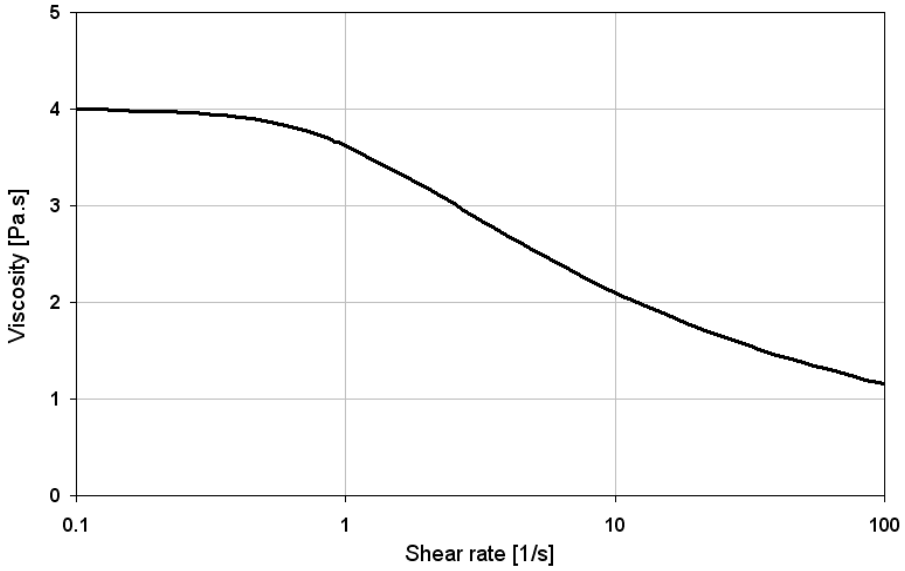

Figure 2.2: Demonstration of viscosity variation as function of shear rate for a shear-thinning fluid.

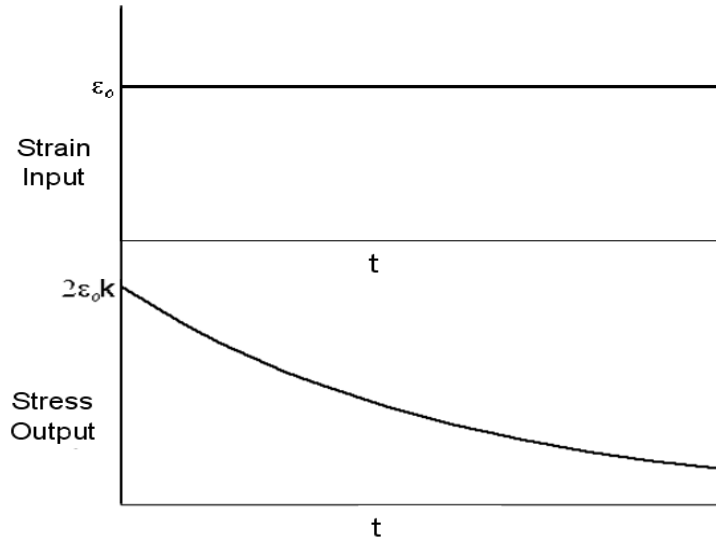

Figure 2.3: Demonstration of stress relaxation in a viscoelastic material.

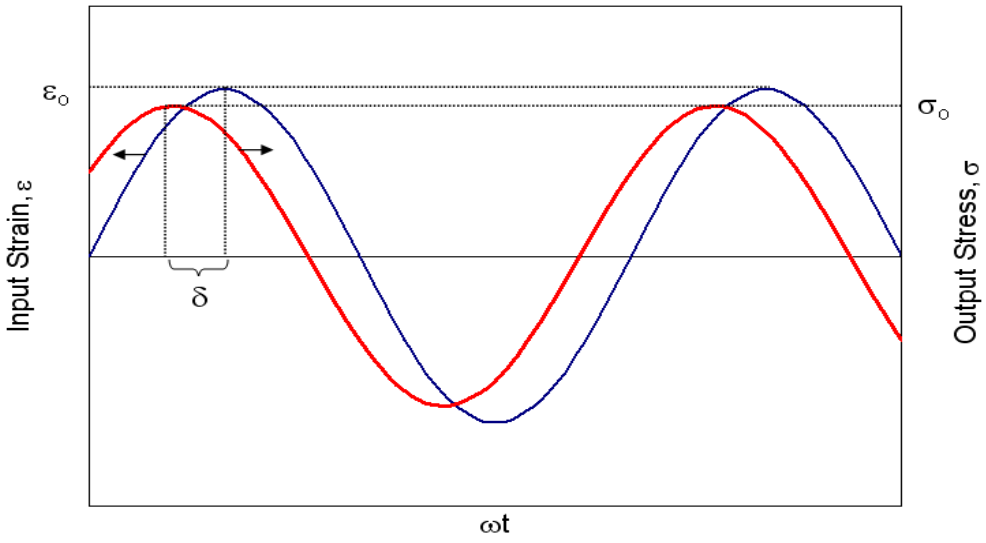

Figure 2.4: Stress response of a viscoelastic material for a sinusoidal strain input.

Chapter 3: Review of Particle Settling in Viscoelastic Fluids

3.1 UNBOUNDED PARTICLE SETTLING

The settling velocity of single spherical particle in a Newtonian fluid in the creeping flow regime was first derived by Stokes in 1851, which is commonly referred to as the Stokes equation. Subsequent researchers studied the settling at higher Reynolds numbers and presented expressions to calculate the drag force (Proudman and Pearson 1957; Ockendon and Evans 1972). For purely viscous non-Newtonian fluids, an effective or apparent viscosity is used in the corrected Stokes equation in order to calculate the settling velocity of a spherical particle. A wide range of literature is available for the equations for settling velocities of spherical particles in purely viscous Newtonian and non-Newtonian fluids (Novotny 1977; Clark and Quadir 1981; Roodhart 1985; Acharya 1986; Daneshy 1990; Gadde et al. 2004).

On the other hand, the past work on the determination of settling velocities of spherical particles in viscoelastic fluids is not as complete. Guar based gels have been used for in the oil industry for hydraulic fracturing operations for many years. These gels are viscoelastic, exhibiting viscous and elastic properties. Various researchers have observed that the solids transport behavior does not correlate well with the viscosity for these gels. Acharya (1988) performed proppant settling experiments in uncrosslinked and crosslinked HPG and carboxymethyl HPG (CMHPG) gels and concluded that in the creeping flow regime ($Re < 2$) the viscous parameters dictate the proppant settling rate and it is not influenced by fluid elasticity for both non-crosslinked and crosslinked gels. It was pointed out that at higher Reynolds numbers the settling velocities calculated on the basis of viscous parameters of the fluid were lower than experimental settling velocities.

It was concluded that fluid elasticity exerts considerable influence and causes the proppants to settle faster. A correlation was presented to calculate the settling velocity of proppants in gels.

Kruijf and Roodhart (1993) showed that the static proppant settling in borate-crosslinked HPG solutions was not controlled by the viscous modulus, G'' but by the elastic modulus, G' of the fluids. In other words the static settling velocity of proppants was determined by the elastic properties of the gels. Goel et al. (2002) performed proppant settling experiments in non-crosslinked and crosslinked guar gels. They observed that for non-crosslinked gels there was a critical guar concentration above which the settling velocity of the proppants decreases considerably. For crosslinked gels it was observed that the solids transport behavior correlated better with the elastic modulus rather than the viscosity. It was also observed that drag coefficients in crosslinked gels were dissimilar at three different pHs because of the difference in the crosslinked networks.

Apart from guar gels, a significant amount of work has been done to study particle settling in other viscoelastic fluids for various applications ranging from semi-conductor processing to pharmaceutical manufacturing. Chhabra et al. (1980) performed experiments in Boger fluids (constant viscosity elastic fluids) and observed an increase in the settling velocity due to the elastic effects. They observed a decrease in the drag coefficient with increasing values of Weissenberg number (dimensionless number used as a measure of elasticity) which reaches an asymptotic value at higher Weissenberg numbers. The Weissenberg number is defined as follows:

$$\mathrm{We} = \frac{2TV}{d_p} \tag{3.1}$$

where T is the relaxation time of the fluid, V is the settling velocity in the fluid and d_p is the diameter of the spherical particle.

Brule and Gheissary (1993) performed experiments with Boger fluids (constant viscosity elastic fluids) as well as shear-thinning viscoelastic fluids, formed by mixing small amounts of polyacrylamide in glucose syrup, and observed that the settling velocity was reduced due to the elastic effects in the fluid. This effect became more pronounced with increasing shear rates experienced by the falling sphere. They did not observe the velocity increase reported by Chhabra et al. (1980).

Walters and Tanner (1992) presented a review of the experimental as well as theoretical studies to determine the drag coefficient for spheres settling in viscoelastic fluids. They discuss the class of viscoelastic fluids known as Boger fluids, which are elastic fluids with a constant shear viscosity. It was shown that for these fluids elasticity causes a reduction in drag with increasing Weissenberg number which is followed by a drag increase at higher Weissenberg number. They also highlight the other important effects observed during the investigation of particle settling in viscoelastic fluids. These included the velocity overshoot effect in which it was shown that particles released from rest can attain velocities up to three times higher than the final terminal velocities. Another important effect discussed was the time effect Here the terminal velocity can be strongly dependent on the time interval between the dropping of successive particles.

McKinley (2002) alluded to significant gaps between the theoretical studies and experimental results for the determination of drag on spheres settling in viscoelastic fluids. It was pointed out that for Boger fluids the elastic contribution to the total viscous drag decreases at low Weissenberg numbers. However at high Weissenberg numbers the extensional effects in the wake of the sphere become important resulting in an increase in drag. Chhabra (2007) provides a comprehensive review of the work done over the past years and highlights that there is a significant gap between the theory and experimental practices because most theoretical developments elucidate the effect of fluid viscoelasticity on spheres in the absence of shear-thinning effects whereas most experimental studies pertain to conditions where viscosity is a function of the shear rate. This gap has been narrowed down by performing experiments in Boger fluids but a significant amount of work needs to be done to understand the drag force on particles settling in shear-thinning viscoelastic fluids.

3.2 EFFECT OF CONFINING WALLS ON SETTLING

The fracture walls exert a retardation effect and reduce the settling velocities of the proppants. This effect is quantified in terms of wall factor, F_w which is defined as the ratio of the settling velocity in the presence of the confining walls to the unbounded settling velocity in the same fluid. Faxen (1923) used the method of reflections to determine the wall factors as a function of ratio of particle diameter to the spacing between parallel walls. The wall factor (F_w) is defined by the ratio of the settling velocity of the particle in presence of confining walls to the settling velocity of the particle in the unbounded fluid. It was pointed out that for Newtonian fluids in the creeping flow regime, the wall factors depend only on the ratio of particle diameter to slot width, irrespective of the viscosity of the fluid. It was shown that the retardation effect of the

parallel walls increases with increasing ratio of particle diameter to spacing between walls.

Miyamura et al. (1981) formulated a 19th order polynomial to determine the wall factors for spheres settling between two parallel plates in Newtonian fluids. Machac and Lecjaks (1995) conducted experiments with purely viscous shear-thinning (power-law) fluids and showed that the retardation effect of the walls decreases with the decreasing flow behavior index, n of the fluid. In other words increased shear-thinning behavior reduces the retardation effect of the walls. They proposed a correlation to calculate the wall factors in terms of the diameter to wall spacing ratio and the flow behavior index, n. Liu and Sharma (2005) conducted a series of experiments with highly viscous Newtonian fluids and linear guar gels and presented correlations for wall factors as function of the rheology of the fluids. They showed that the effect of the fracture walls in reducing the settling velocity of the proppants becomes significant as the ratio of the proppant diameter to the fracture width increases. It is important to note that all the above mentioned results have been shown for inelastic fluids.

The determination of the wall factors for particles settling in viscoelastic fluids has been an area of ongoing activity for the past three decades. However most of the theoretical as well as experimental work has been focused on the settling of spherical particles inside cylinders due to the two-dimensional nature of the problem. Chhabra et al. (1981) performed experiments with viscoelastic aqueous polymer solutions with different rheologies and determined wall factors for different ratios of particle diameter to cylinder diameter. They provided an empirical correlation to calculate the wall factors as a function of the diameter ratio and Weissenberg number. It was highlighted that the

retardation effects due to the cylinder walls reduces with increasing levels of elasticity of the fluid.

Jones et al. (1994) conducted experiments for spheres settling inside cylinders in Boger fluids and observed that the spheres sometimes have to travel distances equivalent to 20 times the diameter before attaining a terminal velocity. They observed that the magnitude of the overshoot in the velocity decreases as the blockage ratio (ratio of particle to cylinder diameter) increases. It was observed that at a blockage ratio of 0.25 there was a considerable enhancement in drag with the increase in Weissenberg number but the drag enhancement disappeared upon increasing the blockage ratio to 0.5. Navez and Walters (1996) performed experiments in shear-thinning viscoelastic fluids for a blockage ratio of 0.5 and observed that the settling was dominated by the viscosity alone and there was negligible influence of the fluid elasticity.

Huang and Feng (1995) performed numerical simulations in two-dimensional steady flows and used the Oldroyd-B model with a shear rate dependent viscosity to calculate the drag force on the cylinder as a function of the fluid rheology and the wall blockage ratio (ratio of the cylinder diameter to the spacing between walls). They observed that for unbounded flows and flows with small blockage ratios (less than 0.1) the drag on the cylinder was increased by elasticity. On the other hand for flows with higher blockage ratios the trend was completely reversed. In other words increasing elasticity reduced the effect of the blocking walls. It was also observed that increased shear-thinning effects reduced the effect of the walls.

It is important to note that all the work done to determine the wall effects in viscoelastic fluids has been done for spheres settling in cylindrical tubes. No data is available for spheres settling in viscoelastic fluids between parallel walls (fracture walls).

Chapter 4: Experimental Methods

In the current work experiments have been performed for proppant settling in VES fluids under unbounded as well as bounded (between solid walls) conditions. This chapter discusses the properties of the fluid used in this study, the rheological measurements and characterization of the fluids and the experimental methods employed to capture and study the settling of proppants.

4.1 DESCRIPTION OF THE FLUIDS

In this experimental study proppant settling is studied in a two component VES fluid system (Zhang 2002). The fluid consists of an anionic surfactant (sodium xylene sulfonate) as one component (commercially known as FAC-1X) and a cationic surfactant (N,N,N, trimethyl-1-octadecamonium chloride) as the second component (commercially known as FAC-2X). The two components are diluted in distilled water and mixed using an overhead mixer to ensure proper mixing. When the two components are mixed at different concentrations and in different proportions the surfactant mixture forms worm like micelles that yield a variety of different rheological properties. The surfactant mixtures are clear viscoelastic gels capable of suspending proppants. Table 4.1 shows the concentrations of the two components for the different fluid mixtures used in this study. Different concentrations and different ratios of two components are mixed to obtain six different mixtures. The concentrations of the two components are mentioned in the units of "gpt" which stands for gallons per thousand gallons.

4.2 RHEOLOGICAL MEASUREMENTS

Steady shear-viscosity measurements and dynamic oscillatory-shear measurements are made for all the fluid mixtures using the ARES rheometer by TA Instruments shown in Figure 4.1. It is observed that the rheology of the fluids is very sensitive to temperature and care is taken that the rheology of the fluid is measured at the same temperature at which the settling experiments are performed. It is observed that the fluids exhibit shear-thinning behavior. The power-law (K, n) model is fitted to the data in the range of the shear rates encountered by the particles during the settling experiments. The shear rate used is the surface averaged particle shear rate defined as ($2V/d_p$), where V and d_p are the settling velocity and particle diameter respectively. Figures 4.2 through 4.9 show the shear stress and viscosity data as a function of the shear rate for the fluid all the configurations mentioned in Table 4.1.

The dynamic oscillatory-shear measurements (explained in Chapter 2: in section 2.2.3) are made in order to quantify the elasticity of the fluids. These measurements are made over a range of frequencies from 0.1 rad/s to 100 rad/s. The storage modulus, G' and the loss modulus, G'' are measured as a function of angular frequency, ω. Figures 4.10 through 4.17 show the moduli as functions of the angular frequency for all the fluid configurations. The data is used to calculate the ratio of the viscous modulus to the elastic modulus (G''/G') as a function of the angular frequency. Figures 4.18 through 4.25 show the plots for the ratio of the moduli against the angular frequency. It is observed that the ratio decreases with the increase in the angular frequency. The relaxation time, T of the fluid is calculated by fitting the data with Equation (2.7). It is observed that the dynamic modulus data fits the above equation very well for all the fluid samples used in the study. The relaxation times of all the fluid configurations are shown in Table 4.1.

4.3 MEASUREMENT OF SETTLING VELOCITIES IN UNBOUNDED FLUIDS

Glass spheres are used as proppants in the settling experiments. These spheres have smooth surfaces and have diameters ranging from 1mm to 5mm. The particles are selected such that they are near-perfect spheres and their diameters are measured with a high resolution microscope. The settling experiments are performed in containers with diameters at least 25 times the diameter of the particles. This is done to ensure that there is no effect of the confining walls on the settling velocity of the particles. The containers are filled with the VES fluids and a sphere is immersed in the fluid and allowed to settle.

A meter stick is placed alongside the cell and the settling process is captured using a video camera. The recorded video is then used to track the position of the particle and measure the terminal settling velocity. We use a software application called "Tracker 2.0" to get accurate measurements of the settling velocities. The experiments are performed under a temperature controlled environment and the room temperature is measured. The rheological properties of the fluid are measured at the same temperature as the experiments and the density of the fluid is measured using an accurate weighing balance. Experiments are conducted with all the fluid mixtures mentioned in Table 4.1. It can be observed that the Fluids 4 & 5 and Fluids 6 & 7 have the same concentration of the two components. However the experiments with these two mixtures were performed twice at different temperatures resulting in different rheologies.

At least 3 measurements are made for each reported settling velocity under each unique set of conditions. In most cases the experiment is repeated 3 to 4 times to ensure

reproducibility. Error bars provided in the experimental results clearly show the reproducibility of the results and the possible variability in the experimental results.

4.4 MEASUREMENT OF SETTLING VELOCITIES BETWEEN PARALLEL WALLS

Two experimental cells made of Plexiglass are used for performing the experiments. These cells are constructed such that the walls are smooth and perfectly parallel to each other. The width between the walls in the two cells is 3.6 mm and 8 mm respectively. The aspect ratio of the two cells is kept low in order to ensure that there is no effect of the walls orthogonal to the parallel walls. Figure 4.26 shows a schematic of the experimental cell. The experimental cells are filled with the viscoelastic fluid and the particles are immersed in the fluid and allowed to settle between the walls. Particles of diameters varying between 1 mm to 5 mm are used in this setup.

As with the unbounded settling velocity measurements, the settling process is recorded with a high resolution camera and the video is used to measure the terminal settling velocity. Figure 4.27 shows a snapshot of a particle settling inside the experimental cell with the meter stick alongside the cell. Figure 4.28 shows a snapshot from the software application “Tracker 2.0” which shows the position of the particle being tracked at fixed time steps. This data is used to calculate the settling velocity of the particles. Repeated measurements are made as before to ensure reproducibility and to obtain error bars on each measurement.

Table 4.1: Properties of the fluid mixtures along with the temperature at which experiment is performed.

Fluid #	K (Pa.s^n)	n	Relaxation time, T (s)
1	0.363	0.484	0.171
2	0.472	0.389	0.389
3	0.336	0.579	0.555
4	0.785	0.771	0.31
5	0.876	0.7395	0.284
6	2.830	0.9805	0.212
7	2.792	0.9755	0.227
8	23.75	0.9645	2.245

Figure 4.1: ARES rheometer by Texas Instruments. Both the steady-shear and dynamic-oscillatory measurements are made using this rheometer.

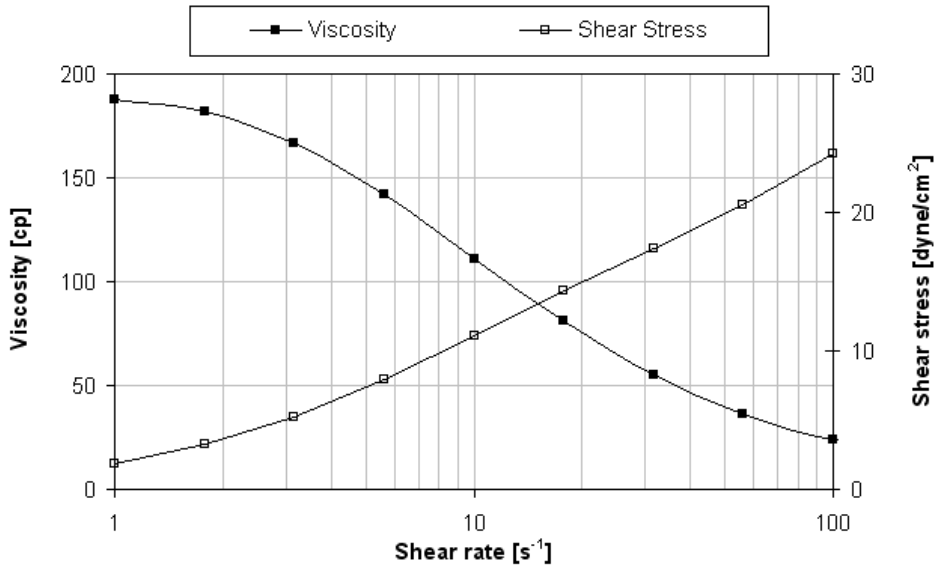

Figure 4.2: Viscosity and shear stress as a function of shear rate for Fluid 1.

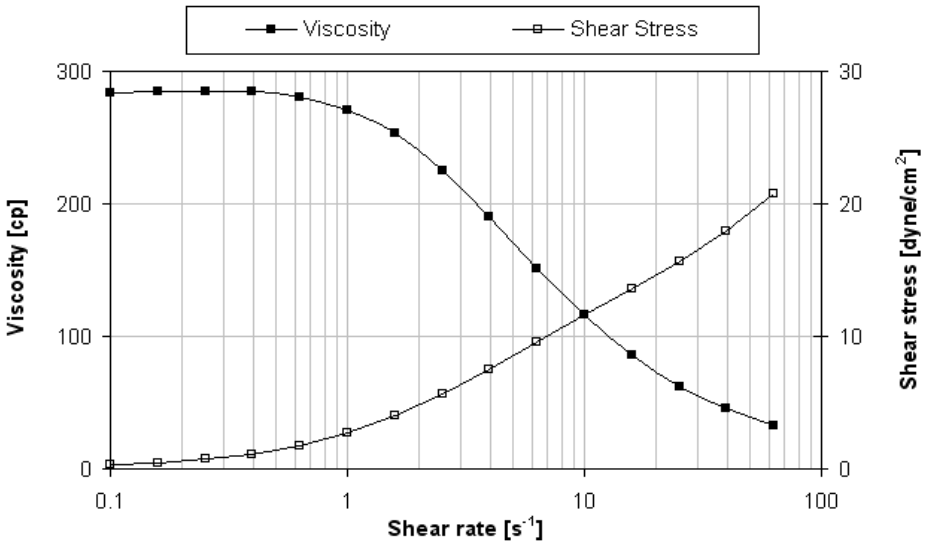

Figure 4.3: Viscosity and shear stress as a function of shear rate for Fluid 2.

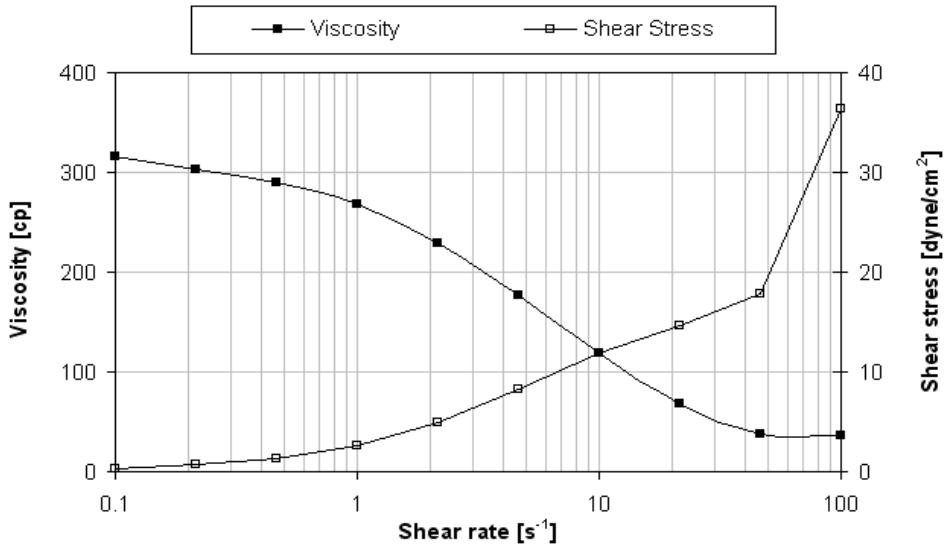

Figure 4.4: Viscosity and shear stress as a function of shear rate for Fluid 3.

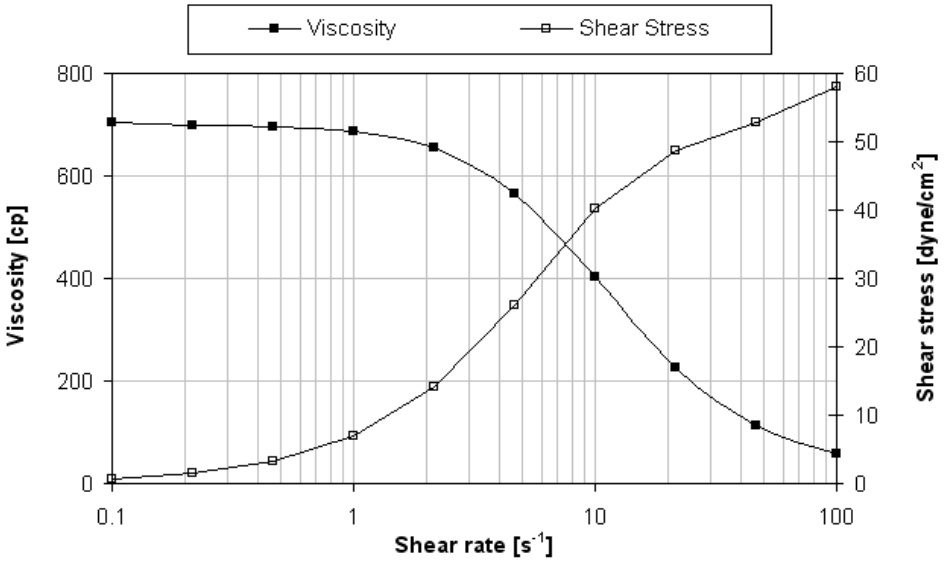

Figure 4.5: Viscosity and shear stress as a function of shear rate for Fluid 4.

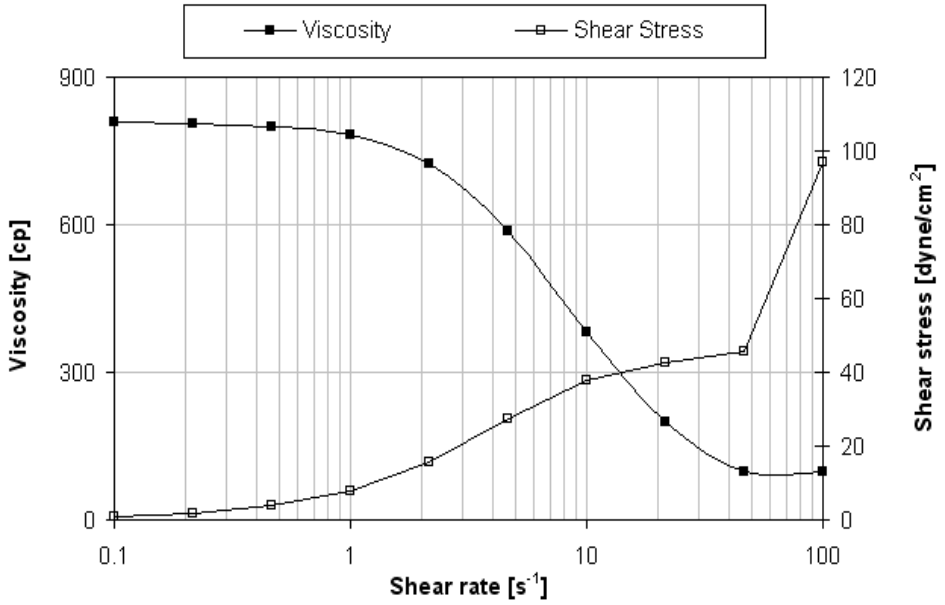

Figure 4.6: Viscosity and shear stress as a function of shear rate for Fluid 5.

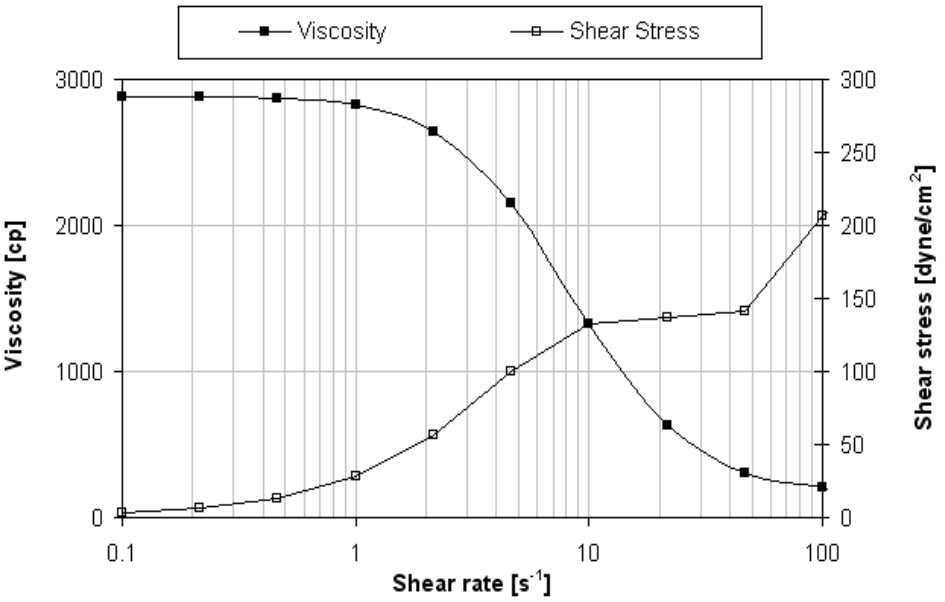

Figure 4.7: Viscosity and shear stress as a function of shear rate for Fluid 6.

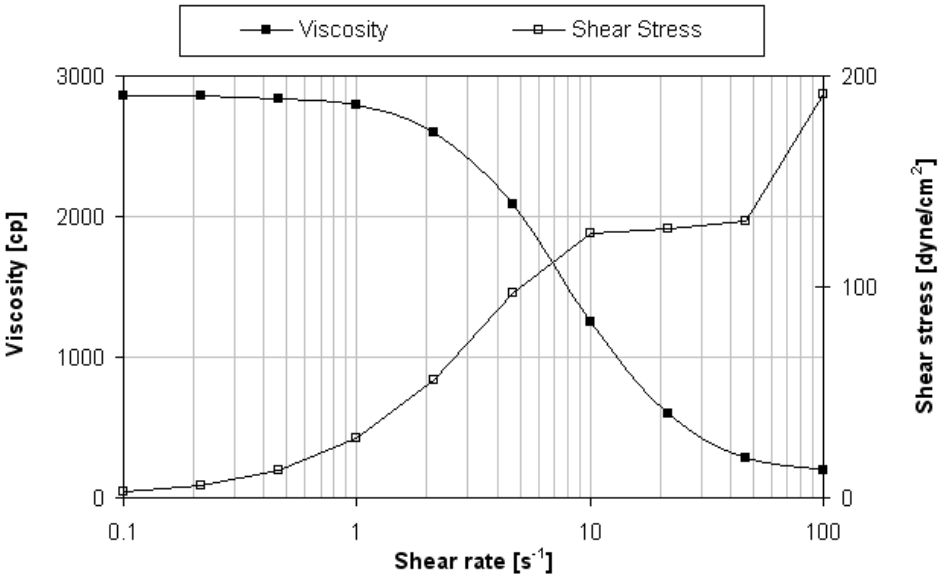

Figure 4.8: Viscosity and shear stress as a function of shear rate for Fluid 7.

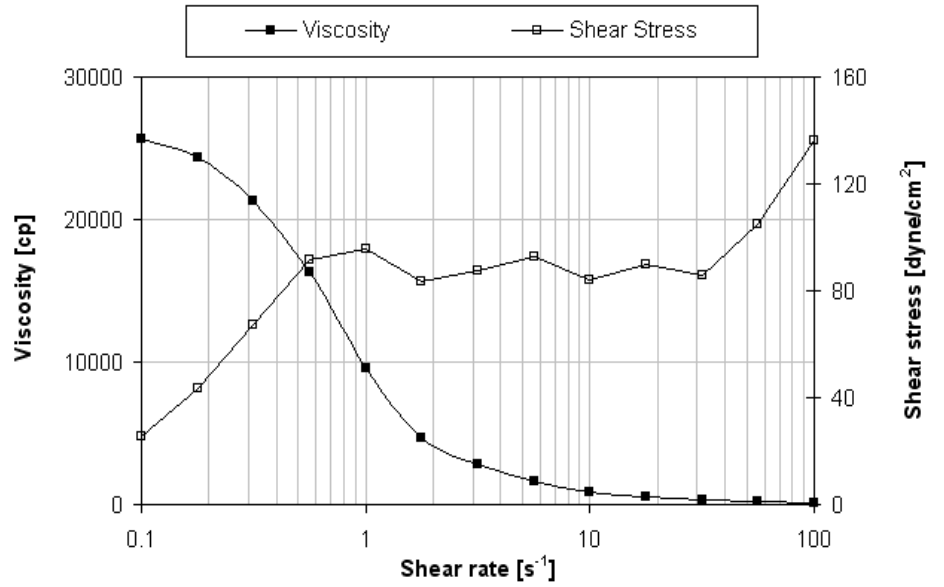

Figure 4.9: Viscosity and shear stress as a function of shear rate for Fluid 8.

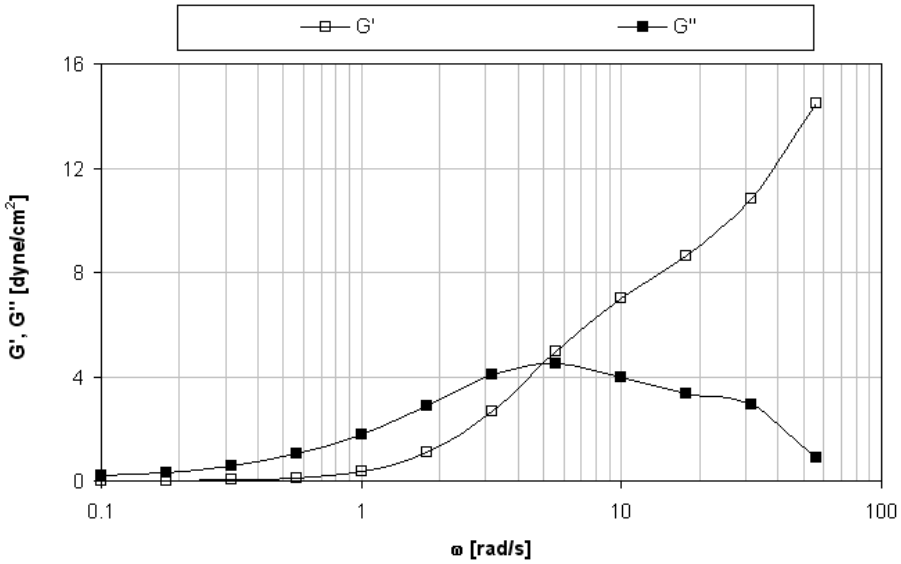

Figure 4.10: Elastic and viscous modulus as a function of angular frequency for Fluid 1.

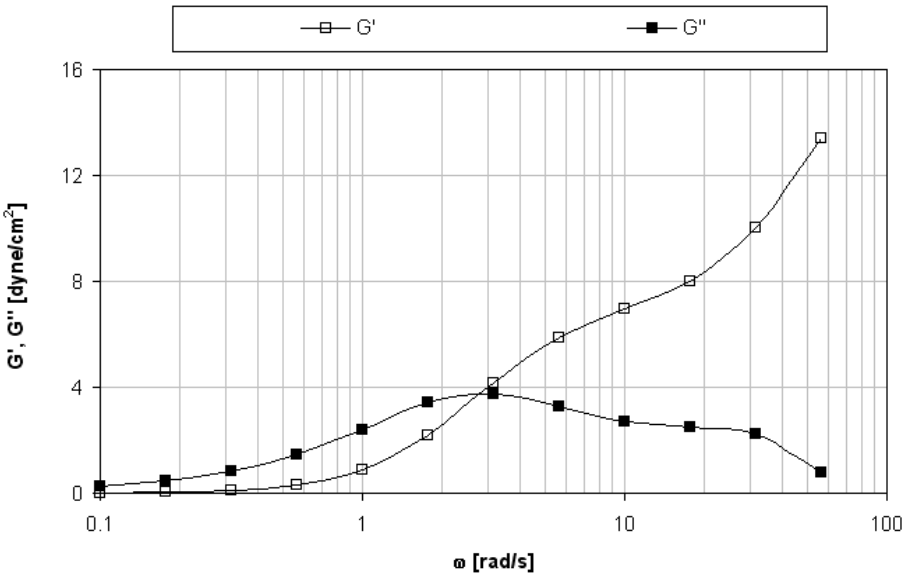

Figure 4.11: Elastic and viscous modulus as a function of angular frequency for Fluid 2.

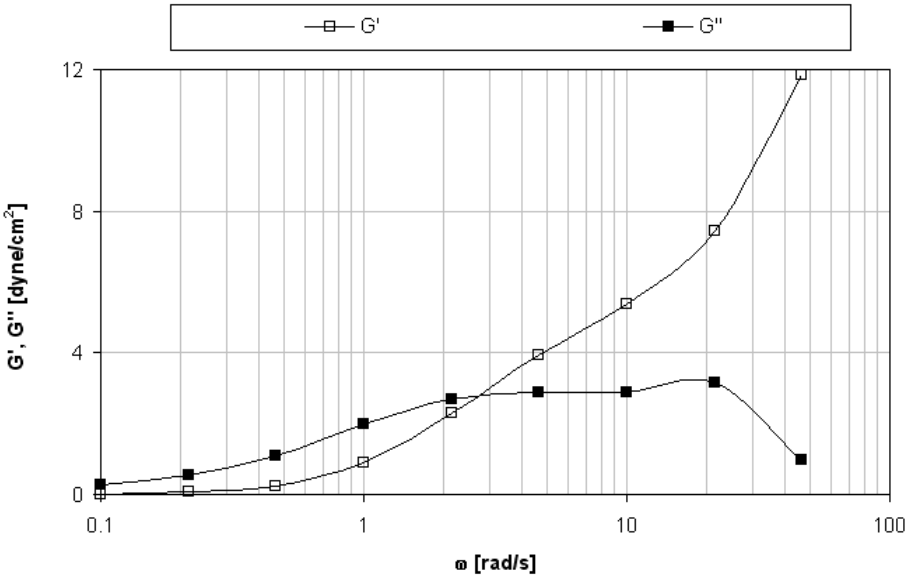

Figure 4.12: Elastic and viscous modulus as a function of angular frequency for Fluid 3.

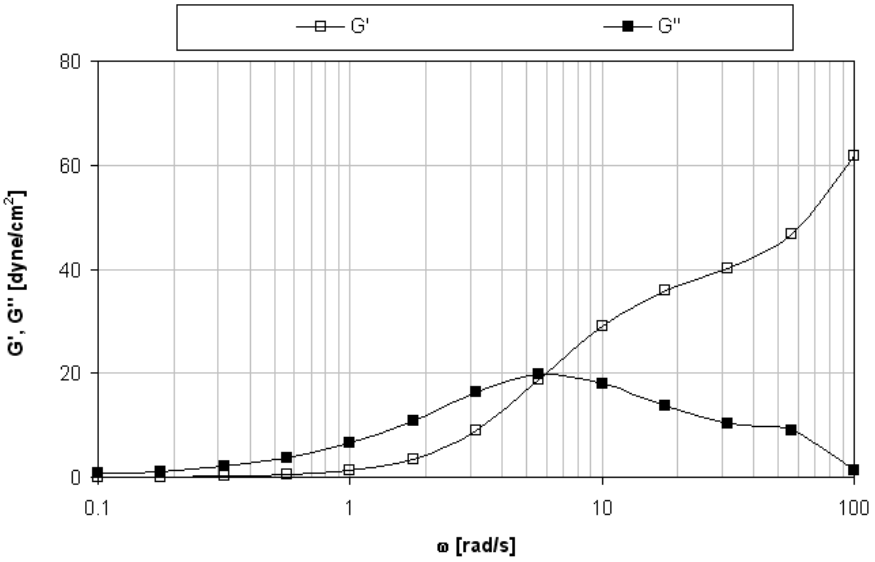

Figure 4.13: Elastic and viscous modulus as a function of angular frequency for Fluid 4.

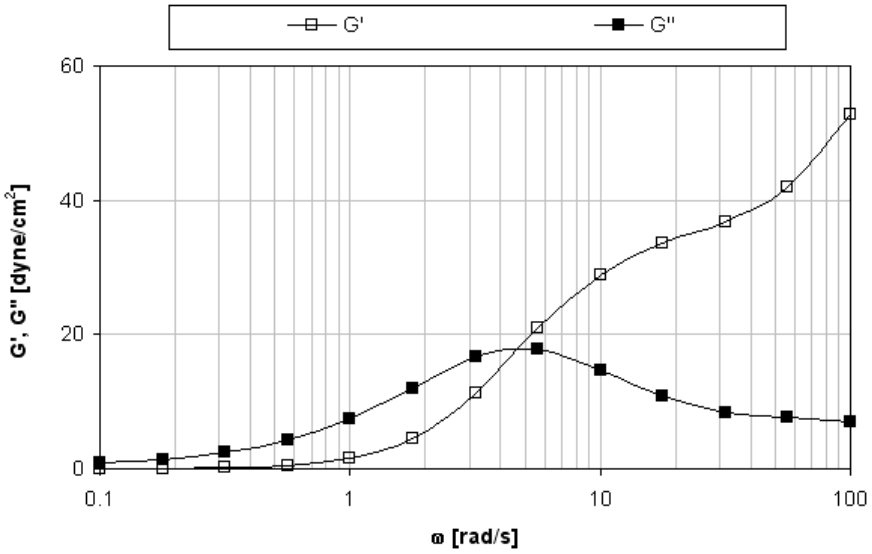

Figure 4.14: Elastic and viscous modulus as a function of angular frequency for Fluid 5.

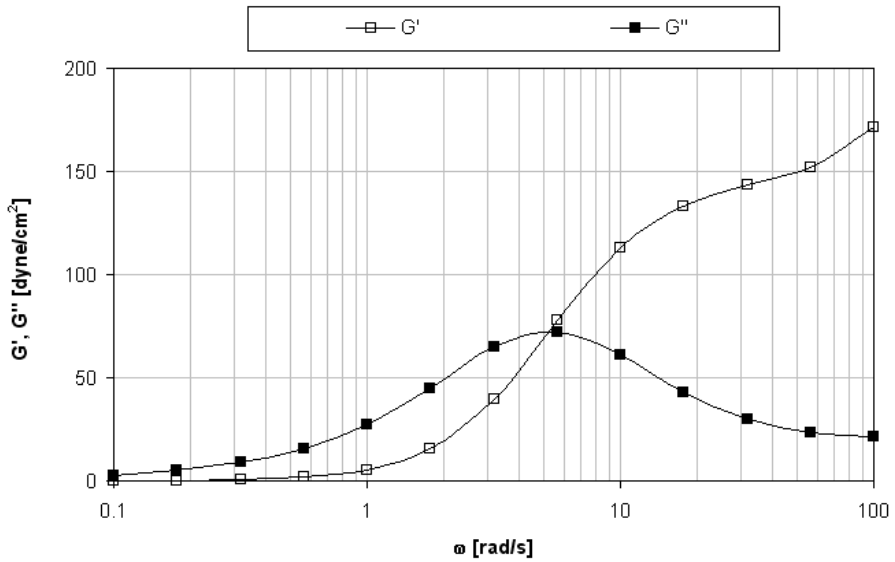

Figure 4.15: Elastic and viscous modulus as a function of angular frequency for Fluid 6.

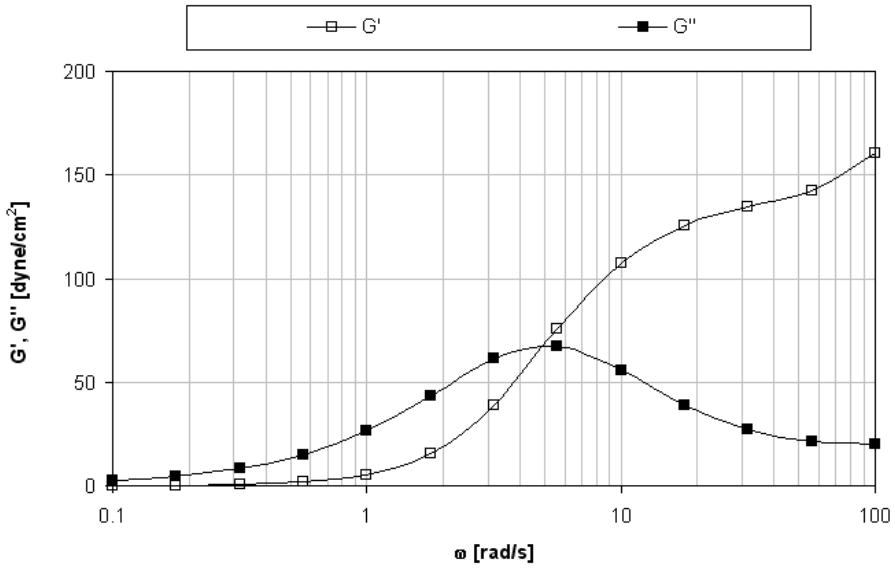

Figure 4.16: Elastic and viscous modulus as a function of angular frequency for Fluid 7.

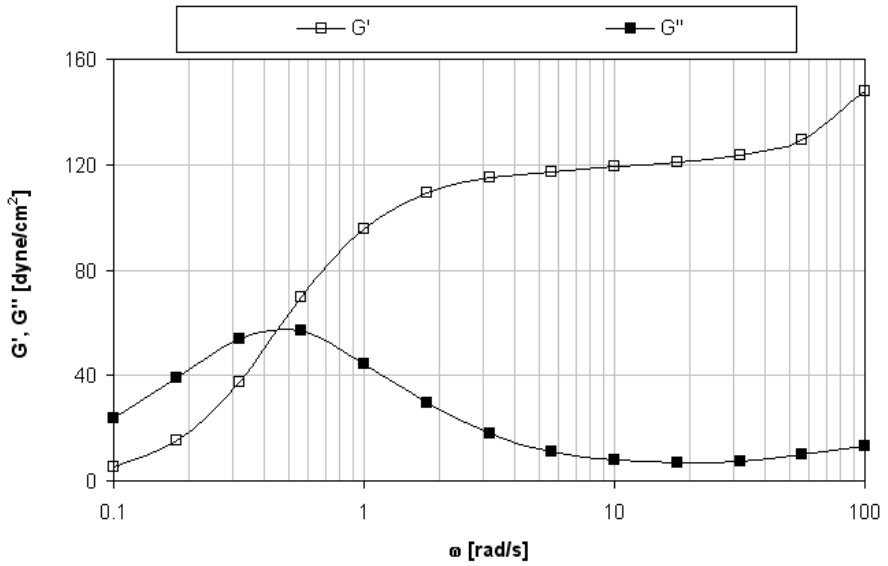

Figure 4.17: Elastic and viscous modulus as a function of angular frequency for Fluid 8.

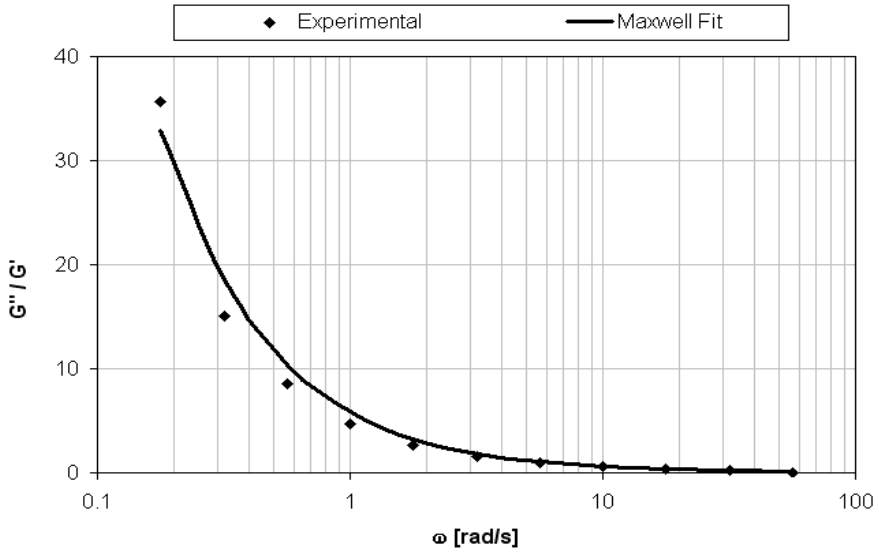

Figure 4.18: Ratio of viscous modulus to elastic modulus for Fluid 1.

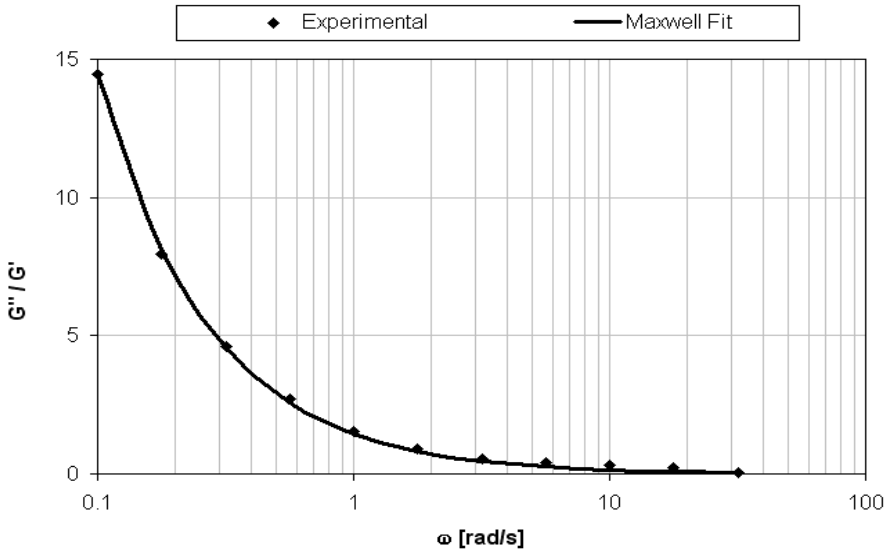

Figure 4.19: Ratio of viscous modulus to elastic modulus for Fluid 2.

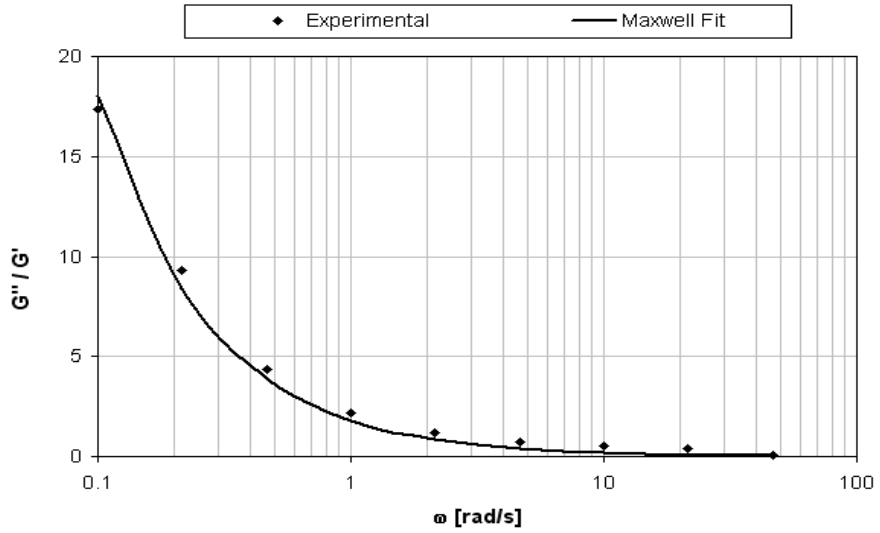

Figure 4.20: Ratio of viscous modulus to elastic modulus for Fluid 3.

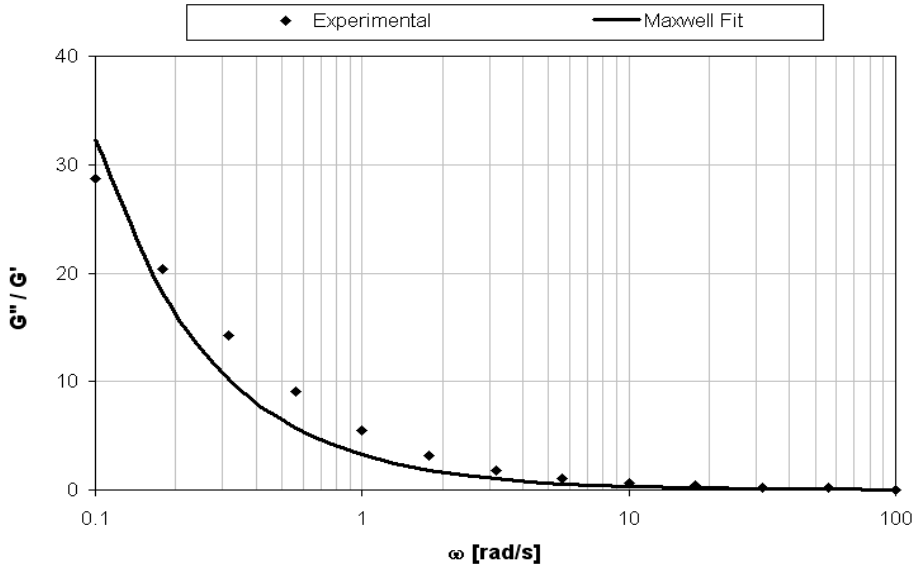

Figure 4.21: Ratio of viscous modulus to elastic modulus for Fluid 4.

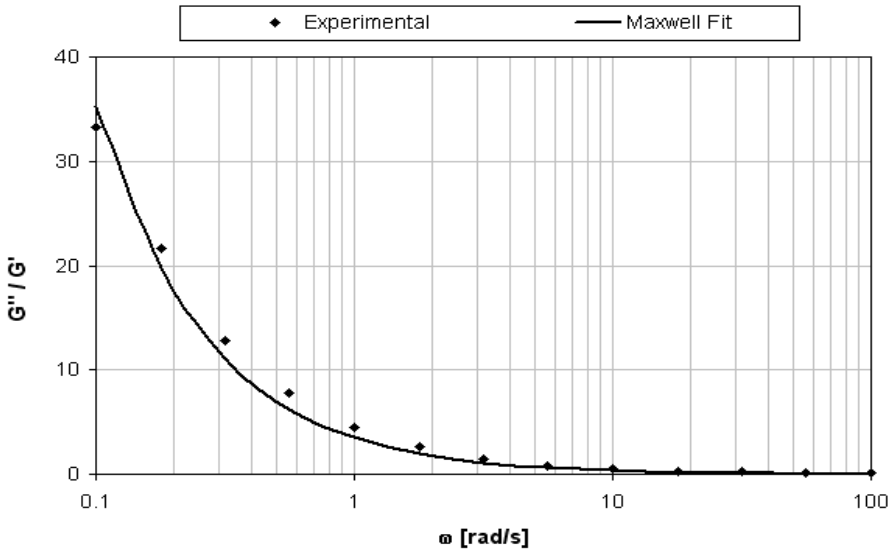

Figure 4.22: Ratio of viscous modulus to elastic modulus for Fluid 5.

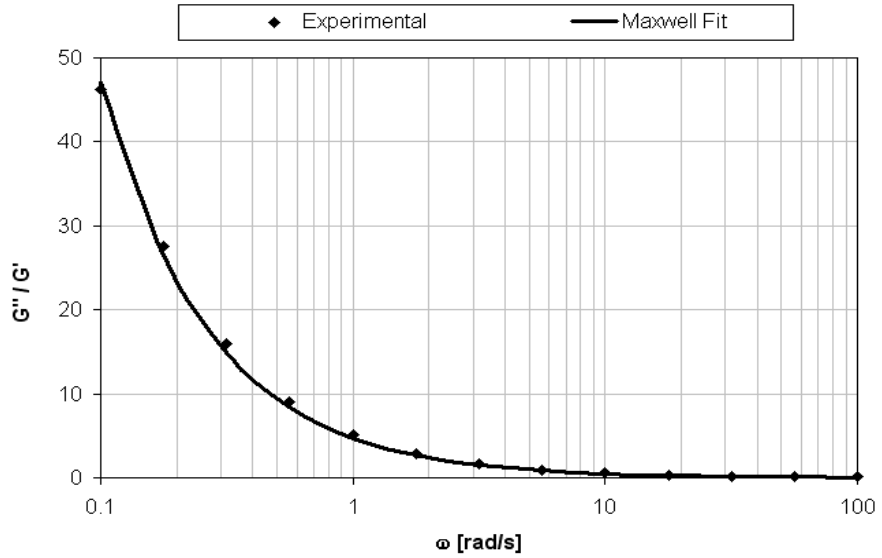

Figure 4.23: Ratio of viscous modulus to elastic modulus for Fluid 6.

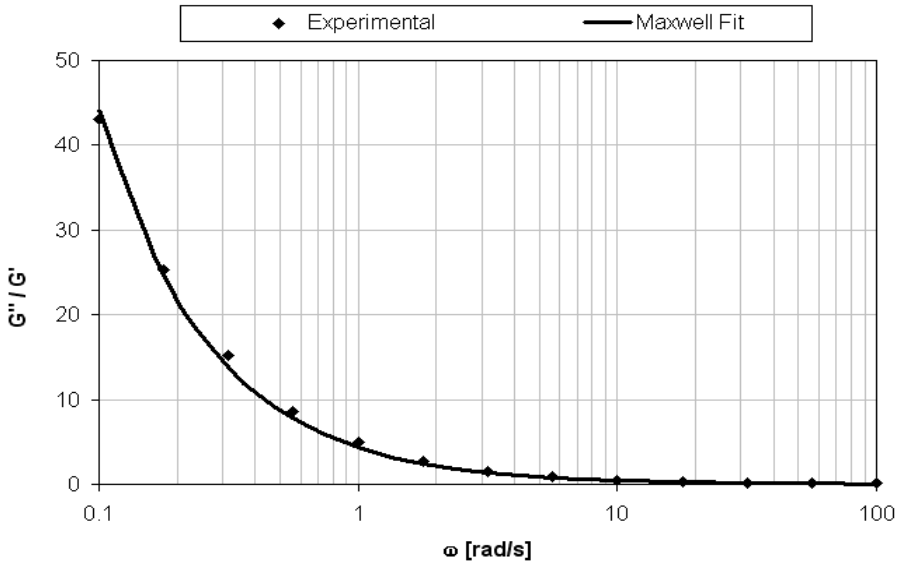

Figure 4.24: Ratio of viscous modulus to elastic modulus for Fluid 7.

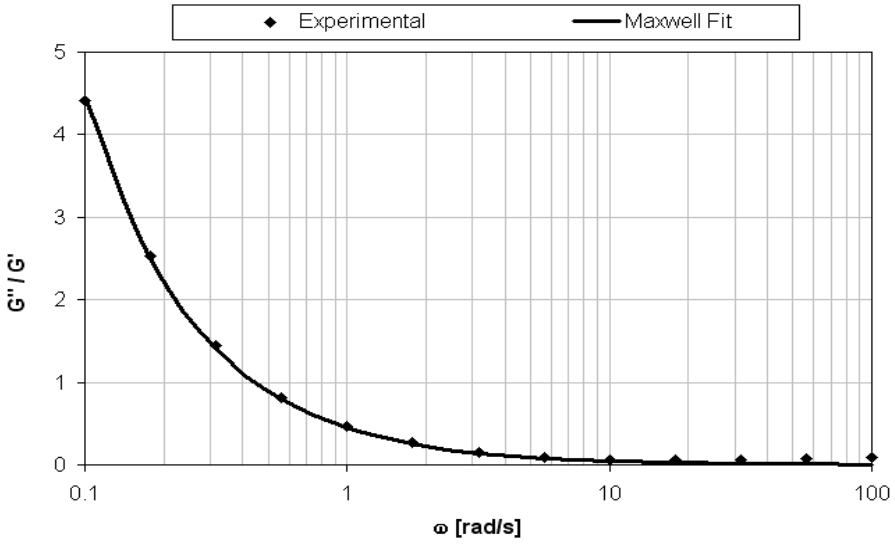

Figure 4.25: Ratio of viscous modulus to elastic modulus for Fluid 8.

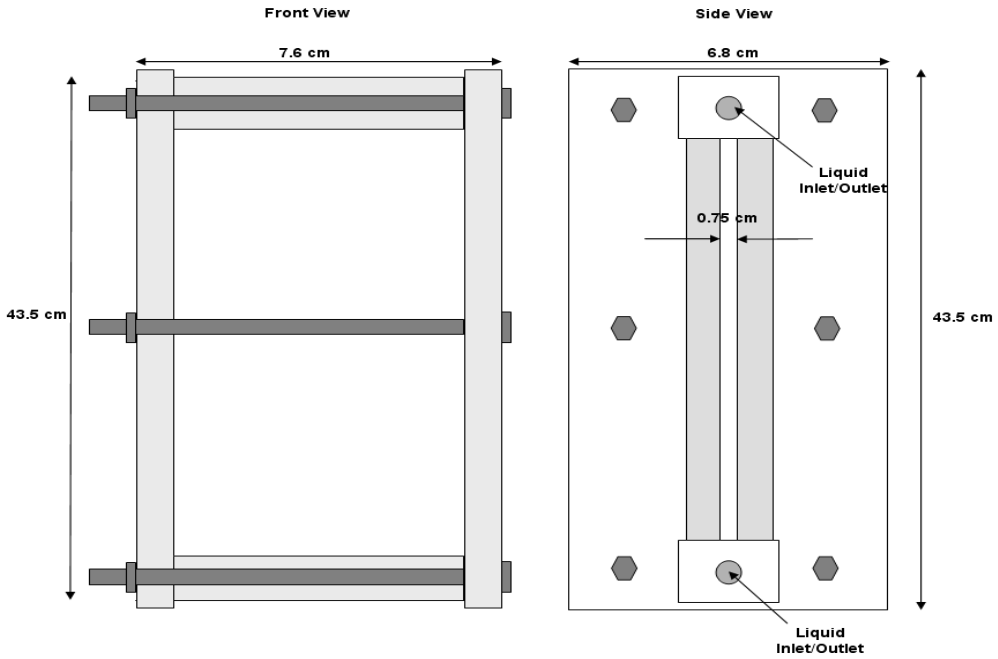

Figure 4.26: Schematic of the experimental cell (not to scale).

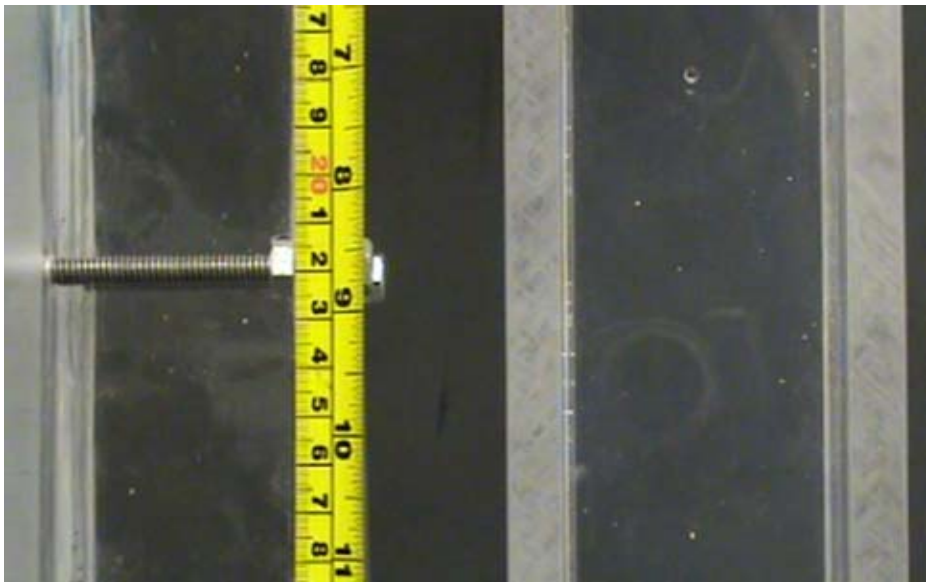

Figure 4.27: Snapshot of the particle settling inside the cell.

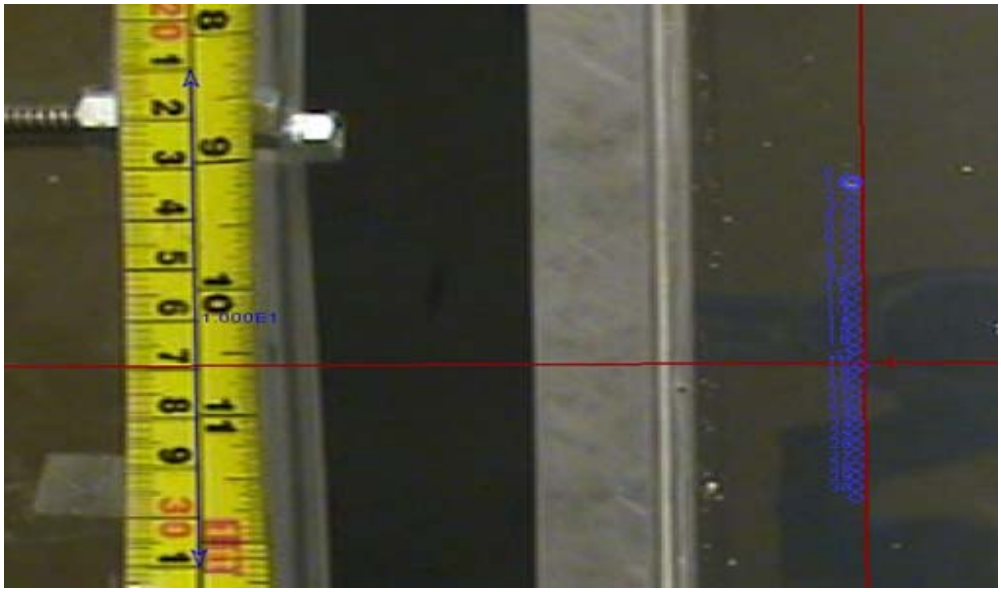

Figure 4.28: Snapshot of the particle tracking process inside the experimental cell using "Tracker 2.0".

Chapter 5: Experimental Observations and Results

5.1 Results For Settling in Unbounded Fluids

Settling velocities in unbounded viscoelastic fluids are experimentally measured for glass spheres of five different diameters in all the eight fluid mixtures mentioned in Table 4.1. Figures 5.1 through 5.8 show the settling velocities as a function of the particle diameter in the eight fluid mixtures. The experimentally measured settling velocity is denoted with the symbol $V_{\infty EL}$ where '∞EL' refers to unconfined viscoelastic fluids. It can be observed that the settling velocity in viscoelastic fluids increase with the diameter of the particle.

This settling velocity is compared with the settling velocity ($V_{\infty INEL}$) calculated on the basis of apparent viscosity data based on the power-law parameters. Here'∞INEL' refers to unconfined inelastic fluids. In other words the experimental settling velocity is compared with the settling velocity of the same spherical particle in an inelastic fluid of the same viscosity. The values of $V_{\infty INEL}$ are calculated using the Equations given below. The following Equations have been obtained from Acharya (1988).

For $Re_{PL} < 2$ (creeping flow regime):

$$V_{\infty INEL} = \left[\frac{(\rho_p - \rho_f)\, g\, d_p^{\,n+1}}{18\, K\, F(n)} \right]^{\frac{1}{n}} \tag{5.1}$$

where *F(n)* is the drag correction factor given by

$$F(n) = 3^{\frac{(3n-3)}{2}}\left[\frac{33n^5 - 63n^4 - 11n^3 + 97n^2 + 16n}{4n^2(n+1)(n+2)(2n+1)}\right] \tag{5.2}$$

For $2 < Re_{PL} < 500$

$$V_{\infty INEL} = \left\{\frac{3\rho_f}{4(\rho_p - \rho_f)gd_p}\left[\frac{24F(n)}{4Re_{PL}} + \frac{f_2(n)}{Re_{PL}^{f_3(n)}}\right]\right\}^{-1/2} \tag{5.3}$$

where

$$f_2(n) = 10.5n - 3.5 \tag{5.4}$$

and

$$f_3(n) = 0.32n - 0.13 \tag{5.5}$$

In the above Equations Re_{PL} is the Reynolds number for a sphere falling in a power law fluid given by:

$$Re_{PL} = \frac{\rho_f V_{\infty INEL}^{2-n} d_p^{n}}{K} \tag{5.6}$$

In other words the Re_{PL} is calculated based on only the viscous properties of these fluids and the settling velocity, $V_{\infty INEL}$ calculated using Equations 5.1 through 5.5. Tables 5.1 through 5.8 show the values of the Re_{PL} calculated from using the above equation for different diameter particles settling in all the eight fluid mixtures.

Any deviation of the experimental settling velocity ($V_{\infty EL}$) from the inelastic settling velocity ($V_{\infty INEL}$) is due to the influence of the elasticity of the fluid. This deviation from the inelastic settling velocity is expressed in terms of velocity ratio, which is the ratio of the $V_{\infty EL}$ to $V_{\infty INEL}$. A ratio greater than 1 suggests an increase in settling velocity due to elasticity and vice versa.

Figure 5.9 shows the variation of velocity ratio as a function of the diameter for Fluid 1. It is observed that the velocity ratio is greater than 1 for the two smaller particles and greater than 1 for the three larger particles. This suggests that the settling velocity is increased by elasticity for the two smaller particles and it is reduced by elasticity for three larger particles. These results indicate that the settling velocity of particles in viscoelastic fluids is not determined by viscosity alone and elasticity plays a role on the drag force on the particle. It is also clear from the figure that elasticity of the fluid can increase as well as decrease the settling velocity.

The increase in the settling velocity due to fluid elasticity has been observed earlier (Acharya et al. 1976; Chhabra et al. 1980; Walters and Tanner 1992; McKinley 2002). At lower Weissenberg numbers (or lower relaxation times) there is a virtual elimination of the wake behind the sphere. As the sphere settles most of the energy is dissipated in the wake and consequently there is less dissipation of energy in viscoelastic fluids leading to a reduction in drag and an increase in settling velocity. However at higher Weissenberg numbers the extensional effects in the wake of the sphere become important and the dilatational stresses slow down the settling velocity (Solomon and Muller 1996; McKinely 2002; Chhabra 2007).

It is important to highlight that the increase in settling velocities at lower Weissenberg numbers followed by reduction at higher Weissenberg number has been observed before only for Boger fluids (constant viscosity elastic fluids) and this behavior has not been reported in shear-thinning viscoelastic fluids.

Figures 5.10 through 5.16 show the velocity ratios as a function of the diameter of the particle for Fluids 2 through 8 respectively. It can also be seen that the magnitude of the velocity ratio is different for the same size particles in fluids of different rheologies. This clearly suggests that the increase as well as decrease in the settling velocities is a combined effect of the rheological properties of the fluid and the properties of the spherical particles.

The values of the Reynolds numbers, as mentioned in Tables 5.1 through 5.8, are less than two for most of the cases i.e. most of the particles settle in the creeping flow regime. From Figures 5.9 through 5.16, it is observed that the velocity ratios deviate from a value of one, even in the creeping flow regime. The trend is different from what has been reported in the literature for settling velocity data in non-crosslinked and crosslinked HGP gels (Acharya 1988). For the HPG gels it was observed that the settling velocity was not affected by elasticity in the creeping flow regime i.e. the velocity ratios are equal to one. At higher Reynolds number the settling velocity has been reported to increase due to the elasticity in the HPG gels. Contrary to this, we observe that for VES fluids the elasticity can increase as well as reduce the settling velocity.

5.2 RESULTS FOR SETTLING BETWEEN PARALLEL WALLS

Settling velocities are experimentally measured for glass spheres settling between parallel walls. Multiple measurements are taken so as to get reliable averages and error bars. As discussed in Section 4.4, two experimental cells containing parallel walls are used. The spacing between the parallel walls is 3.6 mm and 8 mm respectively. Different diameter particles are used such that data points are uniformly obtained for the complete range of particle diameter to wall spacing ratio (r) varying from 0 to 1. The settling

velocities are compared with the settling velocities in the same fluid under unbounded conditions and the wall factors defined by the following equation are calculated.

$$F_w = \frac{Settling\ velocity\ with\ confining\ walls}{Settling\ velocity\ in\ unbounded\ fluid} \tag{5.7}$$

Figures 5.17 through 5.23 show the wall factors (F_w) from settling experiments performed in all fluid mixtures 1 through 7. It is observed that at the same value of r the wall factors are different in different fluids, which suggests that the wall factors depend on the rheology of the fluids. It is also seen that the wall factors are not a function of only the diameter to wall spacing ratio. This can be clearly observed from Figures 5.20 and 5.21. We observe two different values of the wall factors at the same value of r from experiments performed in a fluid mixture using cells of different wall spacing. This suggests that, unlike Newtonian fluids, the wall factors in viscoelastic fluids are dependent on the rheology of the fluids, the particle diameter to wall spacing ratio as well as the diameter of the particle.

From Figure 5.20 it can be seen that the wall factor drops to a value below 0.46 as the ratio of particle diameter to slot with increases to 0.82. This signifies 54% reduction in the proppant settling velocity as the fracture with becomes comparable to the proppant diameter. The experimental results show that the fracture walls exert a significant retardation effect on proppant settling.

Table 5.1: Values of Re_{PL} for different diameter particles settling in Fluid 1.

Diameter (mm)	Re_{PL}
1.74	0.122743
2.03	0.270688
2.94	1.810173
3.63	3.575981
4.17	5.834033

Table 5.2: Values of Re_{PL} for different diameter particles settling in Fluid 2.

Diameter (mm)	Re_{PL}
1.74	0.040221
2.03	0.103615
2.94	1.006583
3.63	3.129449
4.17	6.273798

Table 5.3: Values of Re_{PL} for different diameter particles settling in Fluid 3.

Diameter (mm)	Re_{PL}
1.71	0.114172
1.98	0.219322
2.97	1.334205
3.63	2.271912
4.17	3.552659

Table 5.4: Values of Re_{PL} for different diameter particles settling in Fluid 4.

Diameter (mm)	Re_{PL}
1.71	0.007178
1.98	0.01212
2.97	0.051619
3.63	0.105744
4.17	0.173578

Table 5.5: Values of Re_{PL} for different diameter particles settling in Fluid 5.

Diameter (mm)	Re_{PL}
1.74	0.005647
2.03	0.009997
2.94	0.039421
3.63	0.086082
4.17	0.143892

Table 5.6: Values of Re_{PL} for different diameter particles settling in Fluid 6.

Diameter (mm)	Re_{PL}
1.71	0.000462
1.98	0.000722
2.97	0.002476
3.63	0.004558
4.17	0.006948

Table 5.7: Values of Re_{PL} for different diameter particles settling in Fluid 7.

Diameter (mm)	Re_{PL}
1.74	0.000496
2.03	0.000793
2.94	0.002454
3.63	0.004669
4.17	0.007128

Table 5.8: Values of Re_{PL} for different diameter particles settling in Fluid 8.

Diameter (mm)	Re_{PL}
1.74	6.13E-06
2.03	9.84E-06
2.94	3.07E-05
3.63	5.87E-05
4.17	8.99E-05

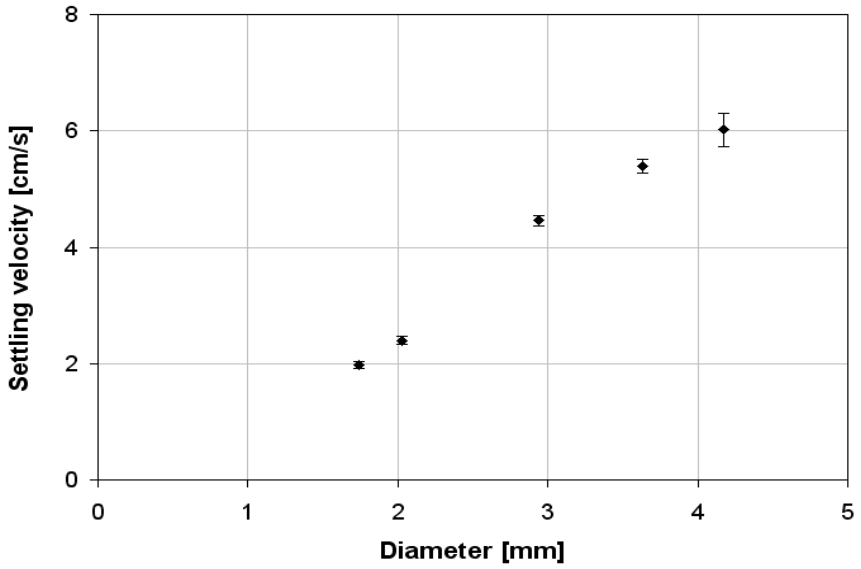

Figure 5.1: Settling velocities in Fluid 1 under unbounded conditions.

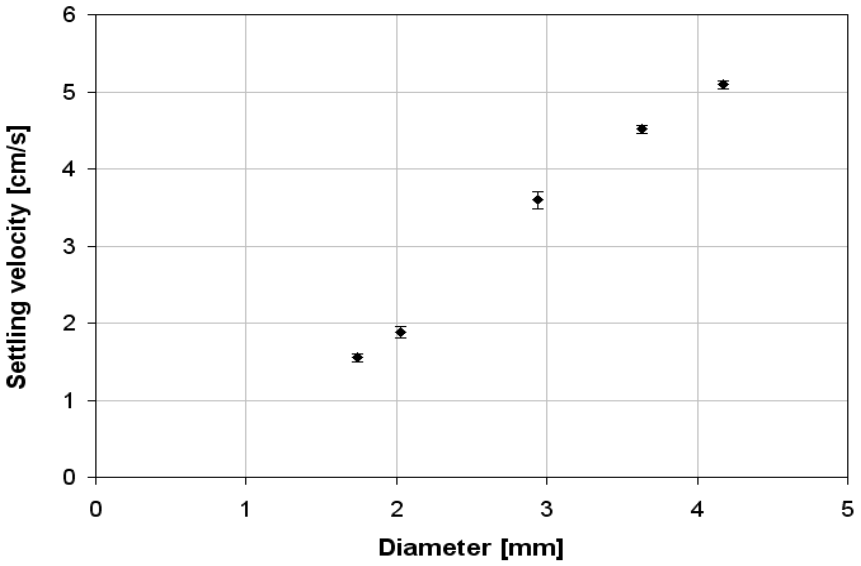

Figure 5.2: Settling velocities in Fluid 2 under unbounded conditions.

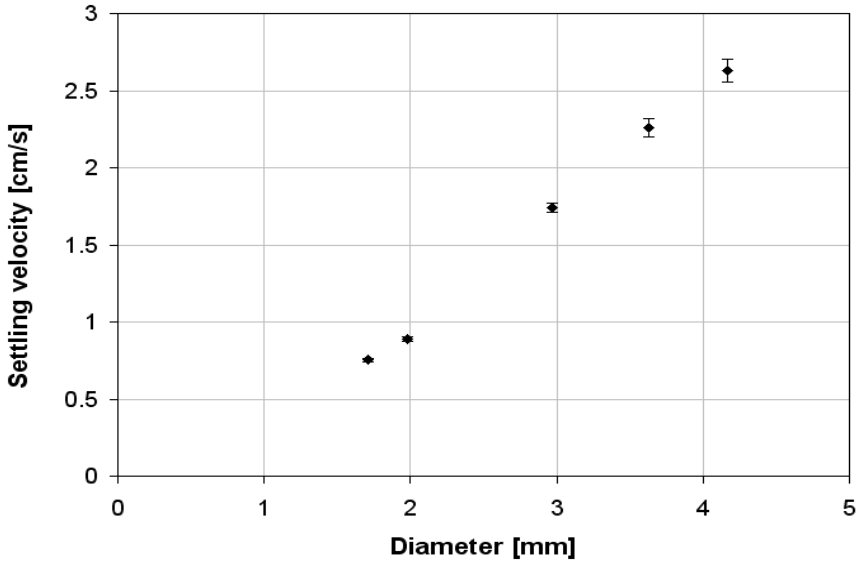

Figure 5.3: Settling velocities in Fluid 3 under unbounded conditions.

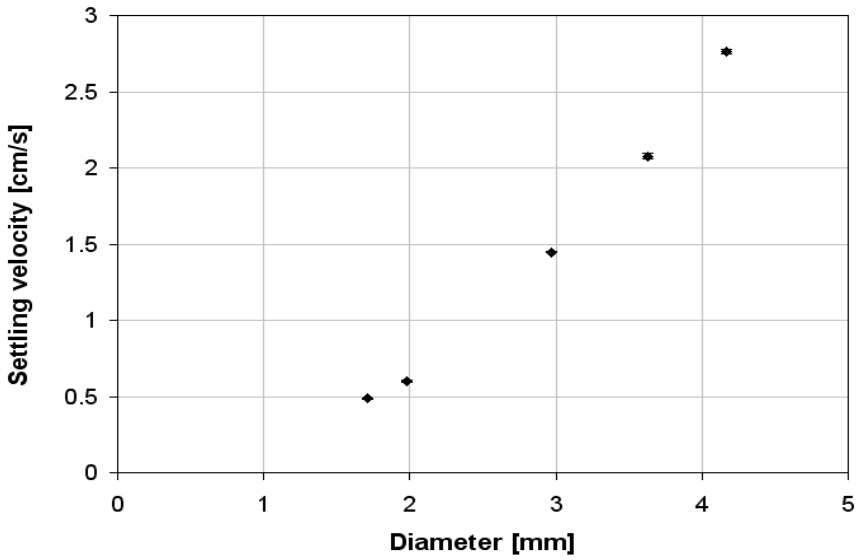

Figure 5.4: Settling velocities in Fluid 4 under unbounded conditions.

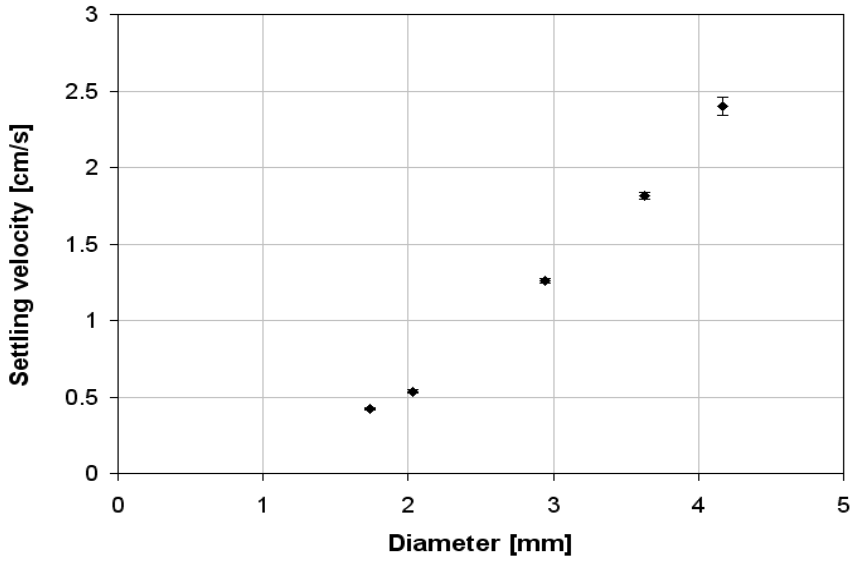

Figure 5.5: Settling velocities in Fluid 5 under unbounded conditions.

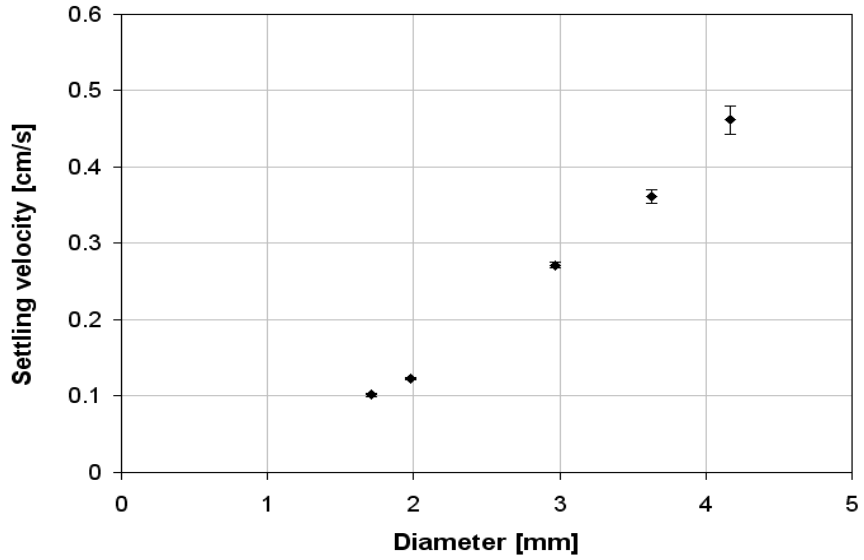

Figure 5.6: Settling velocities in Fluid 6 under unbounded conditions.

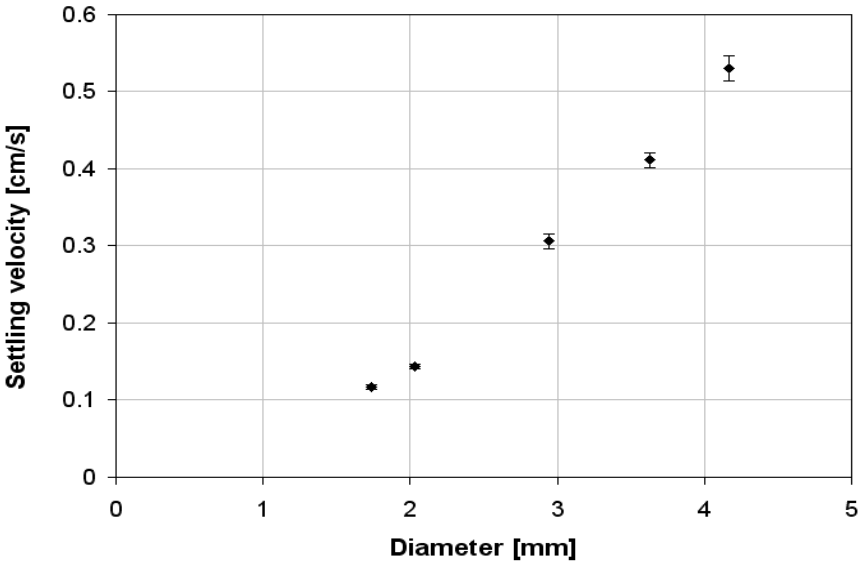

Figure 5.7: Settling velocities in Fluid 7 under unbounded conditions.

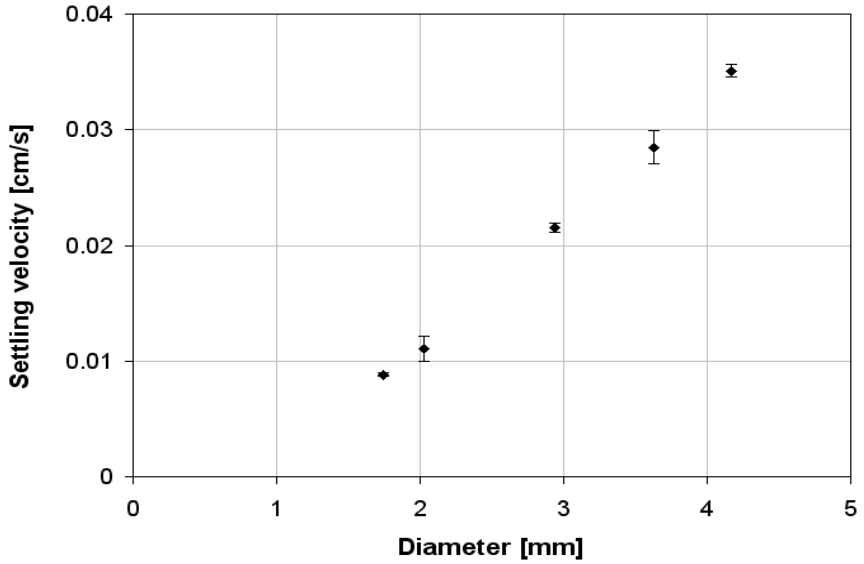

Figure 5.8: Settling velocities in Fluid 8 under unbounded conditions.

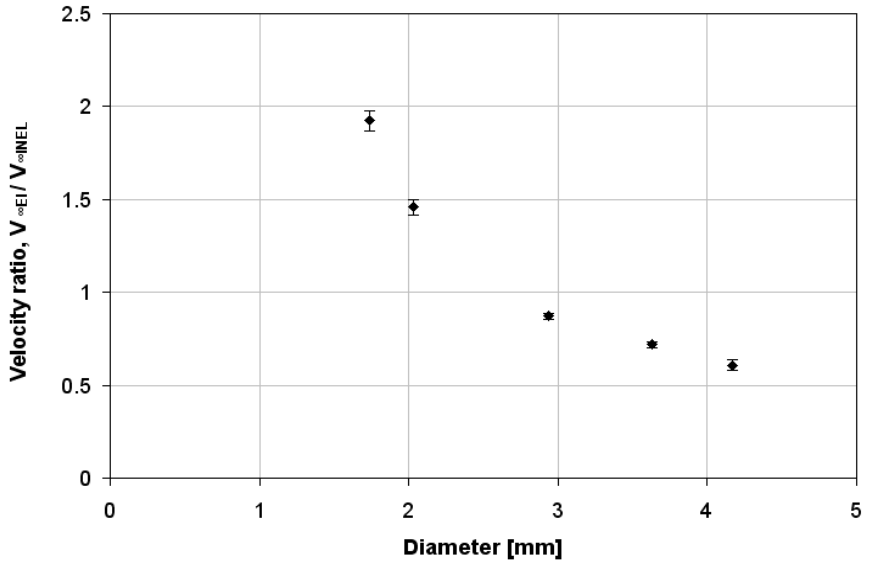

Figure 5.9: Velocity ratios for particles setting in Fluid 1 under unbounded conditions.

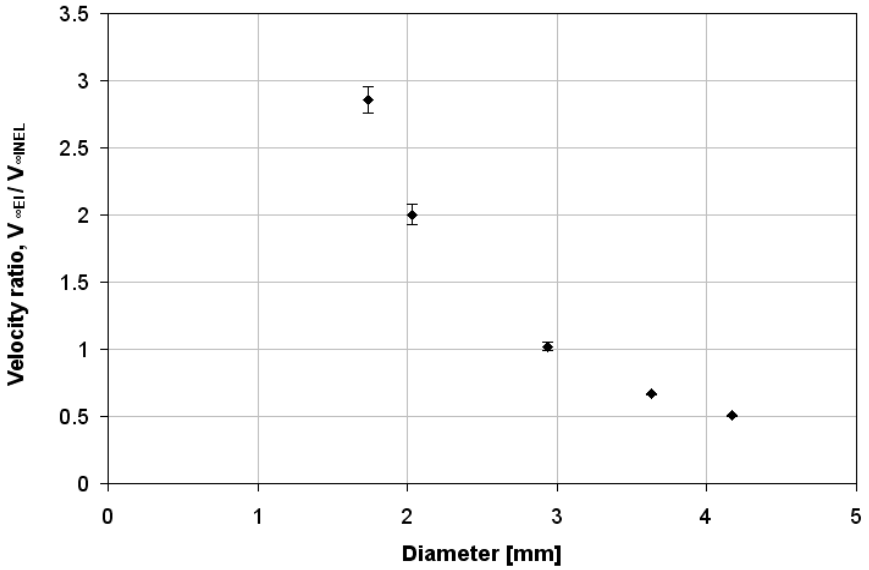

Figure 5.10: Velocity ratios for particles setting in Fluid 2 under unbounded conditions.

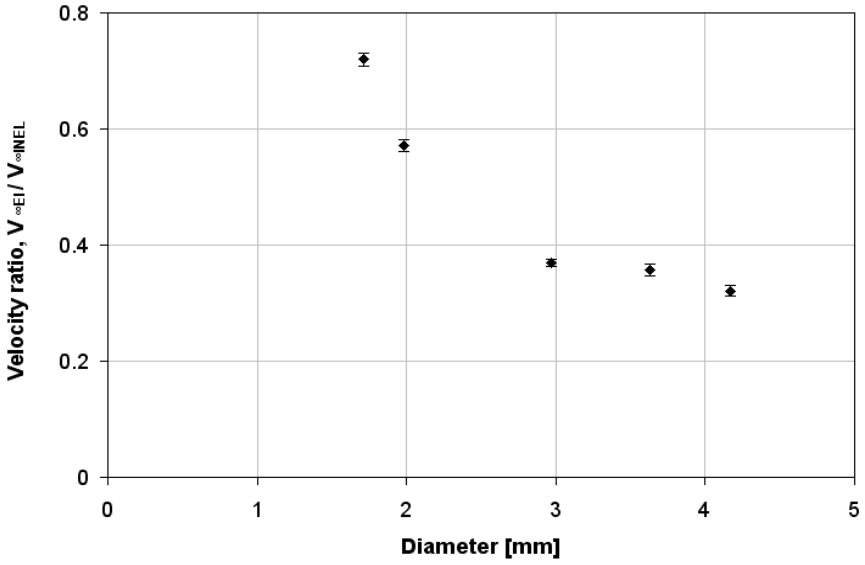

Figure 5.11: Velocity ratios for particles setting in Fluid 3 under unbounded conditions.

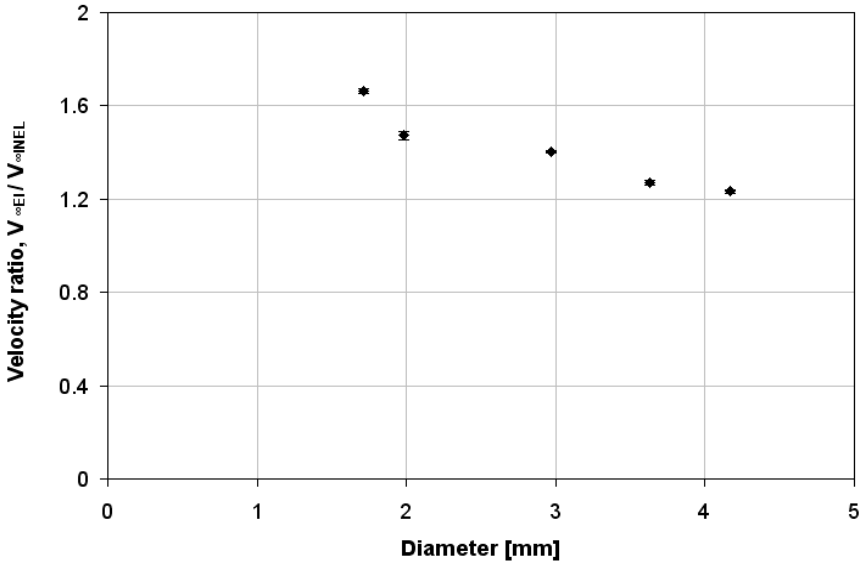

Figure 5.12: Velocity ratios for particles setting in Fluid 4 under unbounded conditions.

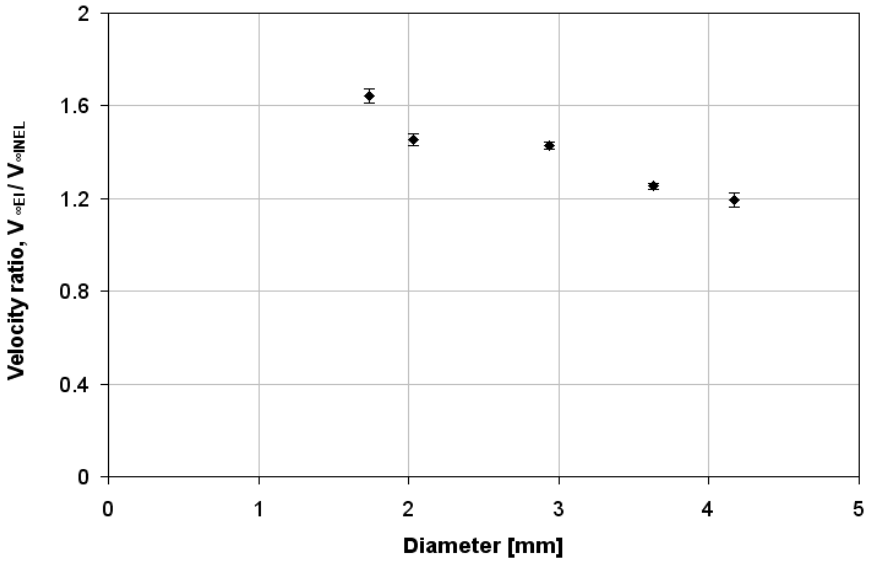

Figure 5.13: Velocity ratios for particles setting in Fluid 5 under unbounded conditions.

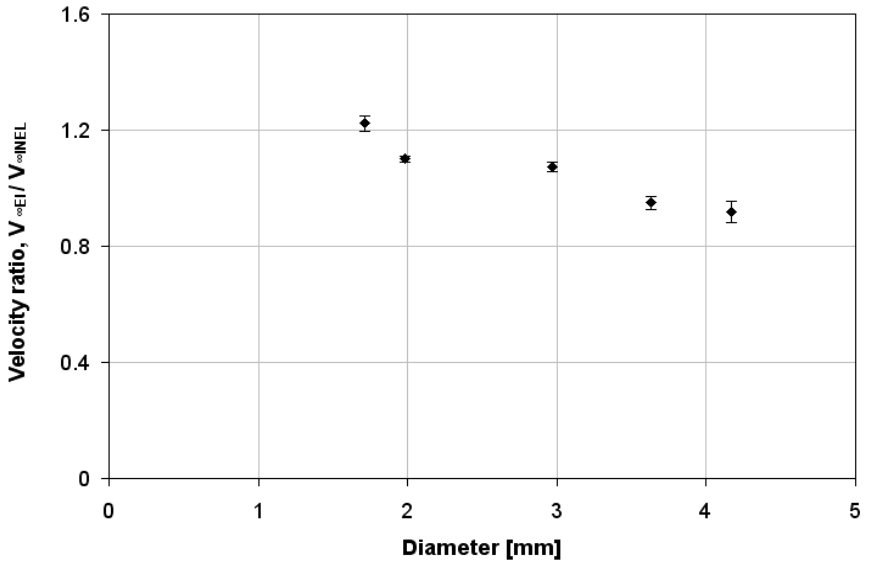

Figure 5.14: Velocity ratios for particles setting in Fluid 6 under unbounded conditions.

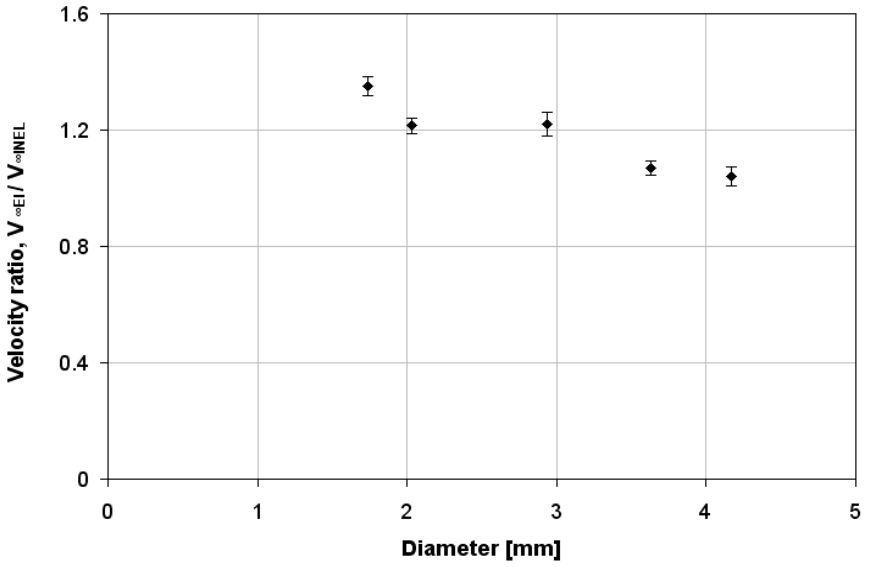

Figure 5.15: Velocity ratios for particles setting in Fluid 7 under unbounded conditions.

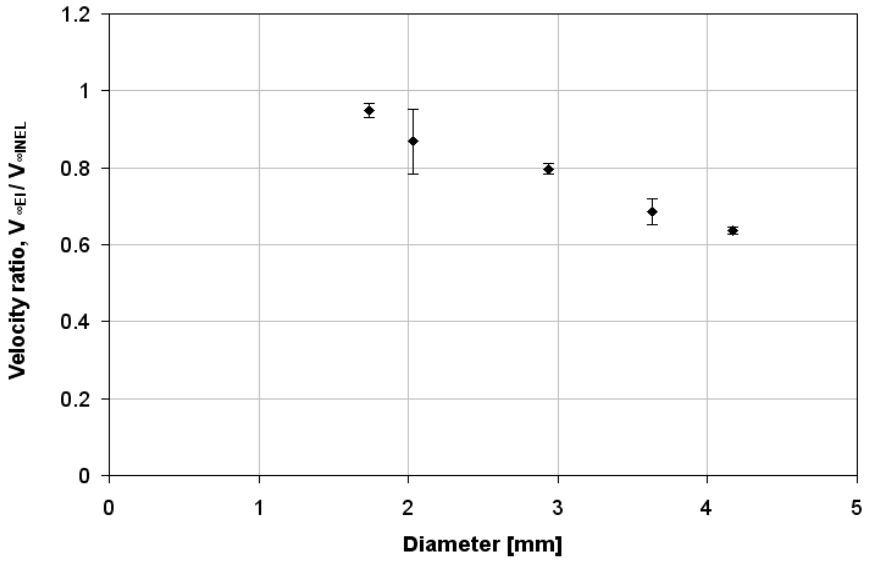

Figure 5.16: Velocity ratios for particles setting in Fluid 8 under unbounded conditions.

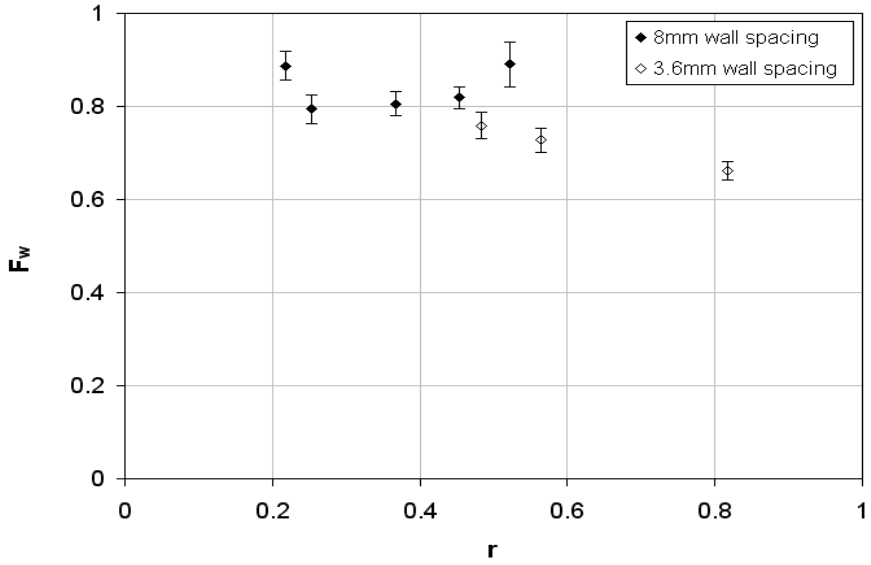

Figure 5.17: Wall factors for particles settling in Fluid 1.

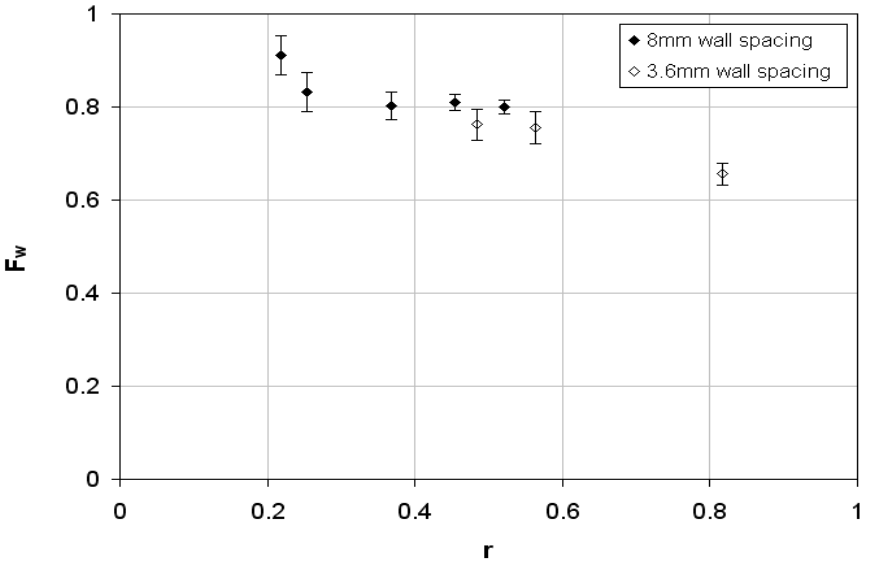

Figure 5.18: Wall factors for particles settling in Fluid 2.

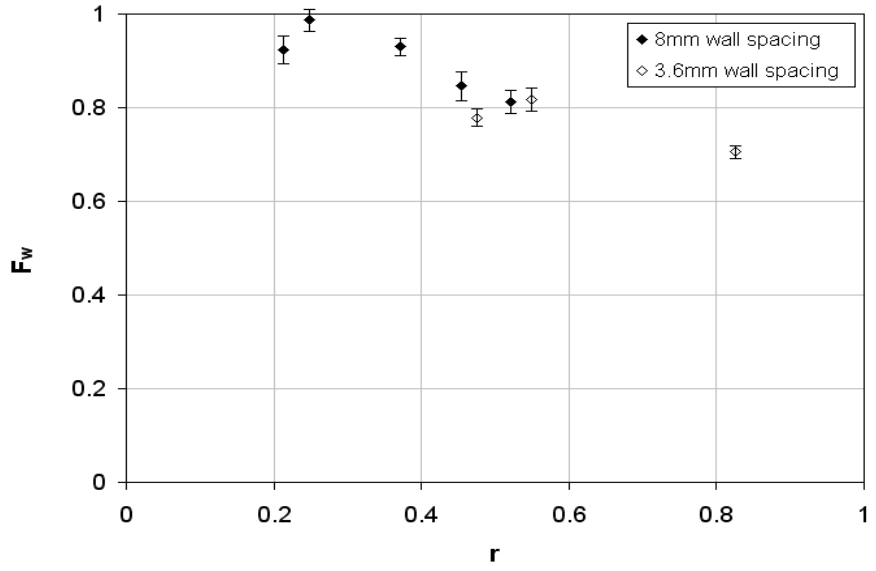

Figure 5.19: Wall factors for particles settling in Fluid 3.

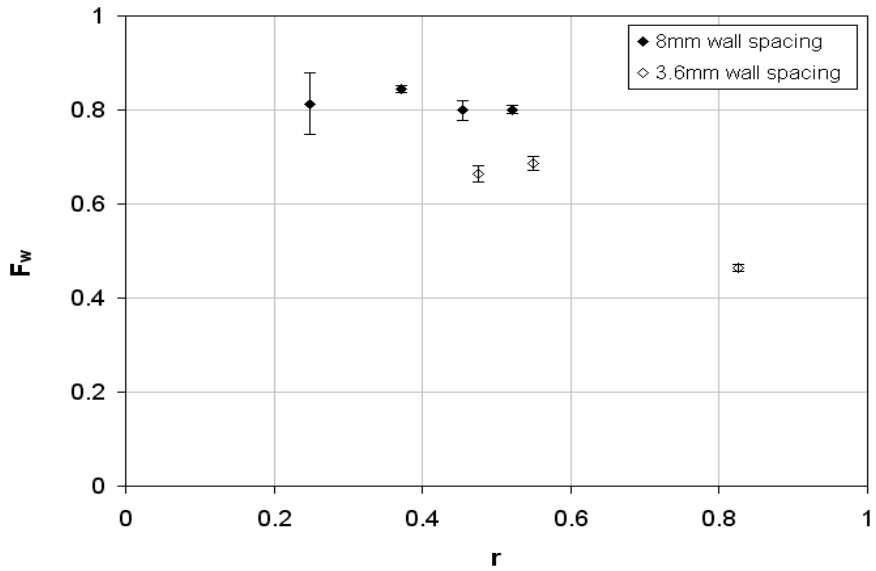

Figure 5.20: Wall factors for particles settling in Fluid 4.

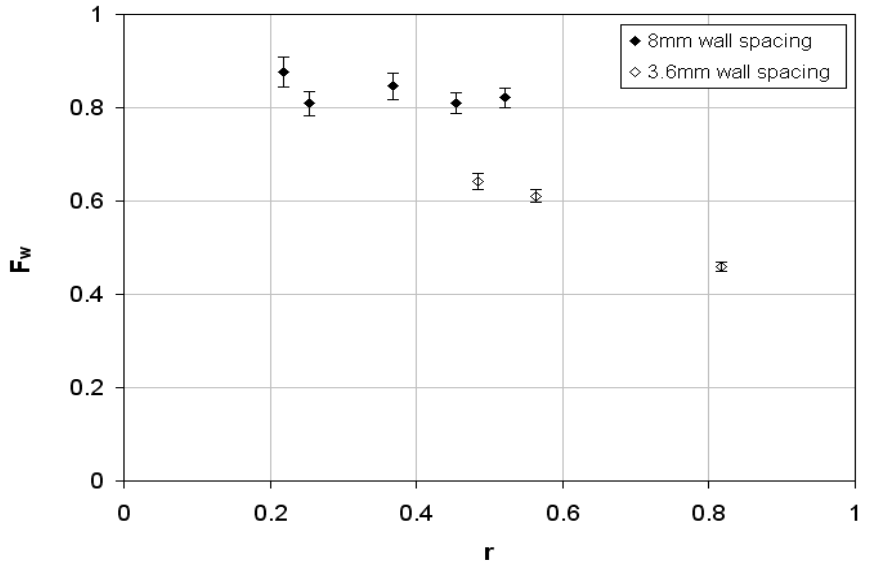

Figure 5.21: Wall factors for particles settling in Fluid 5.

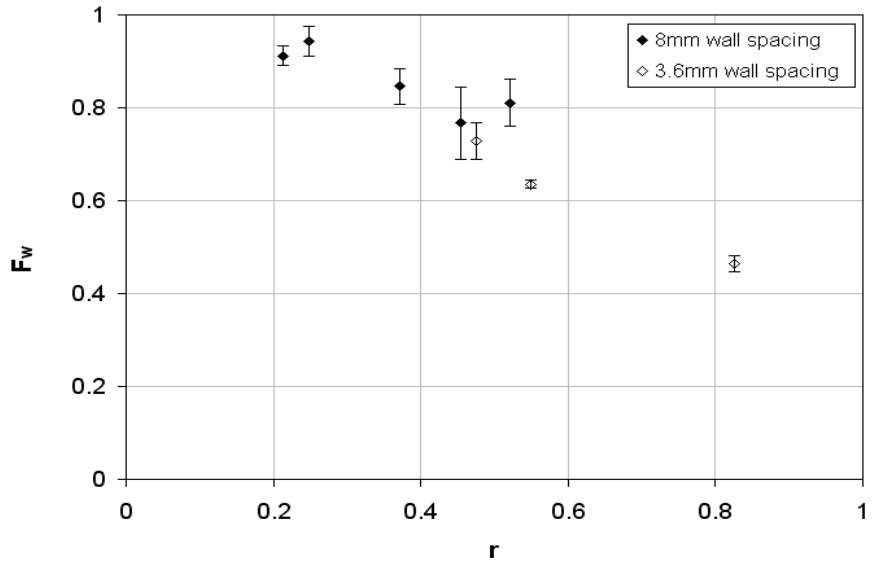

Figure 5.22: Wall factors for particles settling in Fluid 6.

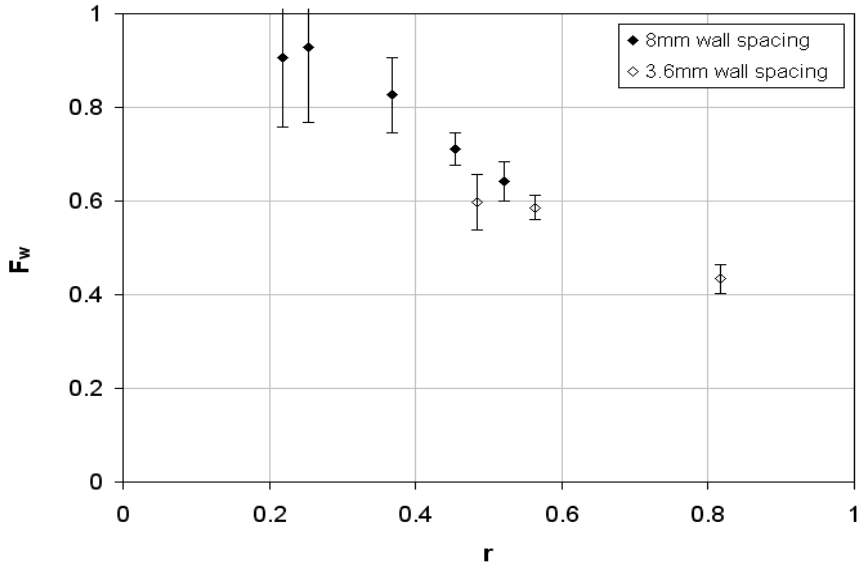

Figure 5.23: Wall factors for particles settling in Fluid 7.

Chapter 6: Conclusions and Future Work

6.1 CONCLUSIONS

This report summarizes the past work that has been performed on determination of drag force on particles settling in viscoelastic fluids and presents results of an experimental study to investigate the settling of spherical particles in shear-thinning viscoelastic fluids. The following conclusions can be drawn from the present study:

- The rheological properties (viscosity and elasticity) of the VES fluid system used in this experimental study are a strong function of the concentration of the two components of the system as well as the fluid temperature. It is observed that the Maxwell model fits the dynamic modulus data accurately and a Maxwellian relaxation time is sufficient to quantify the elastic properties of the fluid system.

- The settling velocity of particles in viscoelastic properties is dependent on the viscosity as well as the elasticity of the fluid, even in the creeping flow regime. The viscous properties alone are not sufficient to determine the drag force on spherical particles in viscoelastic fluids.

- Fluid elasticity can increase as well as decrease the settling velocity of particles. The magnitude of the increase as well as decrease in the settling velocity is dependent on the diameter of the particle as well as the rheological properties of the fluid.

- The confining walls exert a strong retardation effect on the settling velocity of particles in viscoelastic fluids. As the particle diameter approaches the wall spacing the settling velocity reduces considerably.

- It is observed that unlike Newtonian fluids, the wall factors in viscoelastic fluids do not depend on only the diameter to wall spacing ratio. The wall factors are observed to depend on the rheological properties of the fluid, the diameter of the particle and the particle diameter to wall spacing ratio.

6.2 FUTURE WORK

Proper selection of proppants and fracturing fluids for maximum propped fracture length requires reliable data as well as correlations for the impact of fracture fluid viscoelasticity and the effect of fracture walls on proppant settling. The experimental data presented in this report should be used to develop empirical correlations for use in fracture simulators to model proppant transport. The future work for this project entails the following key developments:

- The experimental data for settling velocities and velocity ratios of particles in unbounded VES fluids can be used to develop an empirical correlation to express the settling velocity in terms of the rheological properties of the fluid and the properties of the particle. This empirical correlation should capture the important trends of the velocity ratio variation with the diameter of the particle as shown. It is also important that the analysis should be applicable for settling velocities at different scales and hence a dimensionless analysis is required.

- The correlation will be useful in providing a sensitivity analysis to determine the impact of the individual rheological parameters on the settling velocities of the particles in unbounded VES fluids.

- The wall factors can be expressed in terms of a correlation using the experimental data points. The correlations will be useful in determining the settling velocities of the proppants in the presence of fracture walls and determine the impact of the rheological parameters on the retardation effect due to the walls.

- The experimental correlations can be used in fracture simulators to determine the variation of the settling velocity of the proppants along the length of the fracture. The analysis is essential for proper selection of proppant sizes and design of fracturing fluids.

Nomenclature

d_p = Particle diameter, L, m

$E(t)$ = Relaxation modulus of the sample, m/Lt^2, dyne/cm^2

$F(n)$ = Drag correction factor

$f_2(n)$ = Dimensionless function dependent on the flow behavior index

$f_3(n)$ = Dimensionless function dependent on the flow behavior index

F_w = Wall factor

g = Acceleration due to gravity, L/t^2, m/s^2

G' = Elastic modulus, m/Lt^2, dyne/cm^2

G'' = Viscous modulus, m/Lt^2, dyne/cm^2

k = Spring constant, m/Lt^2, dyne/cm^2

K = Flow consistency index, m/Lt^2-n, Pa.s^n

n = Flow behavior index

r = Ratio of the particle diameter to the fracture spacing

Re = Reynolds number for a sphere settling in a fluid

Re_{PL} = Reynolds number for a sphere falling in an inelastic power-law fluid

T = Relaxation time of the fluid, t, s

t = time after loading the sample, t, s

V = Settling velocity of the proppant inside the fracture, L/t, m/s

$V_{\infty EL}$ = Settling velocity in an elastic unbounded fluid, L/t, m/s

$V_{\infty INEL}$ = Settling velocity calculated on the basis of apparent viscosity in an unbounded fluid, L/t, m/s

We = Weissenberg number of the particle

ω = Angular frequency, 1/t, rad/s

δ = Phase angle expressed in degrees

ρ_f = Density of the fluid, m/L^3, kg/m^3

ρ_p = Density of the particle, m/L^3, kg/m^3

τ = Shear stress, m/Lt^2, $dyne/cm^2$

ε = Strain applied/generated in the sample

ε_o = Constant/Maximum strain applied to the sample

η = Viscosity of the sample, m/Lt, Pa.s

σ = Stress generated in the sample, m/Lt^2, $dyne/cm^2$

σ' = Component of the stress in-phase with the strain, m/Lt^2, $dyne/cm^2$

σ'' = Component of the stress out-of-phase with the strain, m/Lt^2, $dyne/cm^2$

σ_o = Maximum/Amplitude of the stress generated in the sample, m/Lt^2, $dyne/cm^2$

References

Acharya, A., Mashelkar, R.A. and Ulbrecht, J. 1976. Flow of Inelastic and Viscoelastic Fluids past a Sphere: 1. Drag Coefficient in Creeping and Boundary Layer Flows. Rheol. Acta 15: 454-470.

Acharya, A. R. 1986. Particle Transport in Viscous and Viscoelastic Fracturing Fluids. SPEPE, March, p. 104-110.

Acharya, A. R. 1988. Viscoelasticity of Crosslinked Fracturing Fluids and Proppant Transport. SPEPE, November, p. 483-488.

Asadi, M., Conway, M. W. and Barree, R. D. 2002. Zero Shear Viscosity Determination of Fracturing Fluid: An Essential Parameter In Proppant Transport Characterizations. Paper SPE 73755 presented at the SPE International Symposium and Exhibition on Formation Damage Control, Lafayette, Louisiana, 20-21 February.

Brule, B. H. A. A. V. D. and Gheissary, G. 1993. Effects of Fluid Elasticity on the Static and Dynamic Settling of a Spherical Particle. J. Non-Newtonian Fluid Mech. 49: 123-132.

Chhabra, R. P., Uhlherr, P. H. T. and Boger, D. V. 1980. The Influence of Fluid Elasticity on the Drag Coefficient for Creeping Flow Around a Sphere. J. Non-Newtonian Fluid Mech. 6(3-4): 187-199.

Chhabra, R. P., Tiu, C. and Uhlherr, P. H. T. 1981. A Study of Wall Effects on the Motion of a Sphere in Viscoelastic Fluids. Can. J. Chem. Eng. 59: 771-775.

Chhabra, R.P. 2007. Bubbles, Drops and Particles in Non-Newtonian Fluids, second edition, Boca Raton, Florida: Taylor & Francis.

Clark, P. E. and Quadir, J. A. 1981. Prop Transport in Hydraulic Fractures: A Critical Review of Particle Settling Velocity Equations. Paper SPE/DOE 9866 presented at the SPE/DOE Low Permeability Symposium, Denver, Colorado, 27-29 May.

Daneshy, A. 1981. Proppant Transport. In Recent Advances in Hydraulic Fracturing, J. L. Gildley, S. A. Holditch, D. E. Nierodem and R. W. Veatch JR, Chap. 10, Monograph Volume 12, Henry L. Doherty Series, Richardson, TX: Girst Printing.

Dantas, T. N. C., Santanna, V. C., Neto, A. A. D. and Moura M. C. P. A. 2005. Hydraulic Gel Fracturing. J. Dispersion Sci. Tech. 26: 1-4.

Delshad, M., Kim, D. H., Magbagbeola, O. A., Huh, C., Pope, G. A. and Tarahhom, F. 2008. Mechanistic Interpretation and Utilization of Viscoelastic Behavior of Polymer Solution for Improved Polymer-Flood Efficiency. Paper SPE 113620 presented at the SPE Improved Oil Recovery Symposium, Tulsa, Oklahoma, 19-23 April.

Faxen, H. 1923. Der Widerstand gegen die Bewegung einer starren Kugel in einer zähen Flüssigkeit, die zwischen zwei parallelen ebenen Wänden eingeschlossen ist. Ann. Phys. 68: 89-119.

Ferry, J. D. 1970. Viscoelastic Properties of Polymers, second edition, USA: John Wiley & Sons Inc.

Gadde P. B., Liu Y., Norman J., Bonnecaze, R. and Sharma, M. M. 2004. Modeling Proppant Settling in Water-Fracs. Paper SPE 89875 presented at the SPE Annual Technical Conference and Exhibition, Houston, Texas, 26-29 September.

Goel, N., Shah, S. N. and Grady, B. P. 2002. Correlating Viscoelastic Measurements of Fracturing Fluid to Particle Suspension and Solids Transport. J. Pet. Sci. Eng. 35: 59-81.

Gupta, D. V. S. 2009. Unconventional Fracturing Fluids for Tight Gas Reservoirs. Paper SPE 119424 presented at the SPE Hydraulic Fracturing Technology Conference, Houston, Texas, 19-21 January.

Huang, P. Y. and Feng, J. 1995. Wall Effects on the Flow of Viscoelastic Fluids Around a Circular Cylinder. J. Non-Newtonian Fluid Mech. 60: 179-198.

Jones, W. M., Price, A. H. and Walters, K. 1994. The Motion of a Sphere Falling Under Gravity in a Constant Viscosity Elastic Liquid. J. Non-Newtonian Fluid Mech. 53: 175-196.

Kim, D. H., Lee, S., Ahn, C. H., Huh, C. and Pope, G. A. 2010. Development of a Viscoelastic Property Database for EOR Polymers. Paper SPE 129971 presented at the SPE Improved Oil Recovery Symposium, Tulsa, Oklahoma, 24-28 April.

Kruijf, A. S. D., Roodhart, L. P. and Davies, D. R. 1993. Relation Between Chemistry and Flow Mechanics of Borate-Crosslinked Fracturing Fluids. SPEPF, August, p. 165-170.

Leitzell, J. R. 2007. Viscoelastic Surfactants: A New Horizon in Fracturing Fluids for Pennsylvania. Paper SPE 111182 presented at the SPE Eastern Regional Meeting, Lexington, Kentucky, 17-19 October.

Liu, Y. and Sharma, M. M. 2005. Effect of Fracture Width and Fluid Rheology on Proppant Settling and Retardation: An Experimental Study. Paper SPE 96208 presented at the SPE Annual Technical Conference and Exhibition, Dallas, Texas, 9-12 October.

Machac, I. and Lecjaks, Z. 1995. Wall Effect for a Sphere Falling Through a Non-Newtonian Fluid in a Rectangular Duct. Chem. Eng. Sci. 50(1): 143-148.

Mathis, S. P., Pitoni, E., Ripa, G., Ferrara, G., Conte, A. and Ruzic, M. 2002. VES Fluid Allows Minimized Pad Volumes and Viscosity to Optimize Frac-Pack Geometry: Completion Type Evolution in Barbara Field, Central Adriatic Sea. Paper SPE 78317 presented at the SPE European Petroleum Conference, Aberdeen, Scotland, 29-31 October.

McKinely, G. H. 2002. Steady and Transient Motion of Spherical Particles in Viscoelastic Liquids. In Transport Processes in Bubbles, Drops and Particles, ed. D. DeKee and R. P. Chhabra, Chap. 14, second edition, New York: Taylor & Francis.

Miyamura, A., Iwasaki, S. and Ishii, T. 1981. Experimental Wall Correction Factors of Single Solid Spheres in Triangular and Square Cylinders, and Parallel Plates. Int. J. Multiphase Flow 7: 41-46.

Navez, V. and Walters, K. 1996. A Note on Settling in Shear-Thinning Polymer Solutions. J. Non-Newtonian Fluid Mech. 67: 325-334.

Novotny, E. J. 1977. Proppant Transport. Paper SPE 6813 presented at the Annual Technical Conference and Exhibition of the Society of Petroleum Engineers of AIME, Denver, Colorado, 9-12 October.

Ockendon, J. R. and Evans, G. A. 1972. The Drag on a Sphere in Low Reynolds Number Flow, J. Aero. Sci. 3: 237.

Proudman, I. and Pearson, J. R. A. 1957. Expansion at Small Reynolds Number for the Flow Past a Sphere and a Circular Cylinder. J. Fluid Mech. 2: 237.

Roodhart, L. P. 1985. Proppant Settling in Non-Newtonian Fracturing Fluids. Paper SPE 13905 presented at the SPE/DOE Low Permeability Gas Reservoirs, Denver, Colorado, 19-22 May.

Samuel, M., Card, J. C., Nelson, E. B., Brown, J. E., Vinod, P. S., Temple, H. L., Qu, Q. and Fu, K. 1997. Polymer-Free Fluid for Hydraulic Fracturing. Paper SPE 38622 presented at the SPE Annual Technical Conference and Exhibition, San Antonio, Texas, 5-8 October.

Solomon, M. J. and Muller, S. J. 1996. Flow Past a Sphere in Polystyrene-based Boger Fluids: The Effect of the Drag Coefficient of Fluid Extensibility, Solvent Quality and Polymer Molecular Weight. J. Non-Newtonian Fluid Mech. 62: 81-94.

Walters, K. and Tanner, R. I. 1992. The Motion of a Sphere through an Elastic Fluid. In: Transport Processes in Bubbles, Drops and Particles, ed. R. P. Chhabra. and D. DeKee, Chap. 3, New York: Hemisphere.

Zhang, K. 2002. Fluids for Fracturing Subterranean Formations. U.S. Patent No. 6,468,945.